

See discussions, stats, and author profiles for this publication at: <https://www.researchgate.net/publication/6609173>

Heterogeneous dynamics, ageing, and rejuvenating in van der Waals liquids

ARTICLE *in* THE JOURNAL OF CHEMICAL PHYSICS · JANUARY 2007

Impact Factor: 2.95 · DOI: 10.1063/1.2399527 · Source: PubMed

CITATIONS

9

READS

20

2 AUTHORS, INCLUDING:



[Samy Merabia](#)

French National Centre for Scientific Research

47 PUBLICATIONS **515** CITATIONS

SEE PROFILE

Heterogeneous dynamics, ageing, and rejuvenating in van der Waals liquids

Samy Merabia and Didier Long

Citation: *J. Chem. Phys.* **125**, 234901 (2006); doi: 10.1063/1.2399527

View online: <http://dx.doi.org/10.1063/1.2399527>

View Table of Contents: <http://jcp.aip.org/resource/1/JCPSA6/v125/i23>

Published by the [American Institute of Physics](#).

Additional information on J. Chem. Phys.


Journal Homepage: <http://jcp.aip.org/>

Journal Information: http://jcp.aip.org/about/about_the_journal

Top downloads: http://jcp.aip.org/features/most_downloaded

Information for Authors: <http://jcp.aip.org/authors>

ADVERTISEMENT



AIPAdvances

Special Topic Section:
PHYSICS OF CANCER

Why cancer? Why physics? [View Articles Now](#)

Heterogeneous dynamics, ageing, and rejuvenating in van der Waals liquids

Samy Merabia and Didier Long^{a)}

*Laboratoire de Physique des Solides, Université de Paris XI, Bâtiment 510,
91405 Orsay Cédex, France*

(Received 7 August 2006; accepted 24 October 2006; published online 15 December 2006)

It has been shown over the past ten years that the dynamics close to the glass transition is strongly heterogeneous: fast domains coexist with domains three or four decades slower, the size of these regions being about 3 nm at T_g . The authors extend here a model that has been proposed recently for the glass transition in van der Waals liquids. The authors describe in more details the mechanisms of the α relaxation in such liquids. It allows then to interpret physical ageing in van der Waals liquids as the evolution of the density fluctuation distribution towards the equilibrium one. The authors derive the expression of macroscopic quantities (volume, compliance, etc.). Numerical results are compared with experimental data (shape, times to reach equilibrium) for simple thermal histories (quenches, annealings). The authors explain the existence of a “Kovacs memory effect” and the temporal asymmetry between down jump and up jump temperatures experiments, even for systems for which there is no energy barriers. Their model allows also for calculating the evolution of small probe diffusion coefficients during ageing. © 2006 American Institute of Physics. [DOI: 10.1063/1.2399527]

I. INTRODUCTION

When cooling a glass forming liquid, one observes a rapid increase of the viscosity.^{1,2} Usually T_g is arbitrarily defined as the temperature at which the viscosity reaches 10^{12} Pa s in simple liquids, or at which the dominant relaxation time τ_α becomes larger than about $\tau_g \sim 10^2$ s. Typically, the viscosity or the dominant relaxation time increases by 12 orders of magnitude between $T_g + 100$ K and T_g , and their evolution over this temperature range is described by the VFT law (or WLF law in the context of polymer).³ When cooling a glass forming liquid down to lower temperatures, the system no longer reaches thermodynamical equilibrium on the experimental time scale. The point of view that we adopt in this paper is that the glass transition is a dynamical phenomenon, characterized by a rapid increase of the relaxation times of the liquid, without referring to a possible thermodynamic transition.¹ Because liquids below T_g are out-of-equilibrium systems, their physical properties evolve with time. This process is called ageing. It can last for an experimentally accessible duration until the system reaches equilibrium, or last for months and years or more.^{4–8} During this process, the relaxation times of the samples increase with the ageing time, which results, e.g., in a decrease of the compliance of the system. The model that we describe here is intended for van der Waals liquids, whether molecular or polymeric liquids. The temperature range will be typically comprised between $T_g + 80$ K and $T_g - 30$ K. One may consider that for temperatures above $T_g - 10$ K the system can relax towards equilibrium (in about a few 10^4 s at $T_g - 10$ K), whereas below $T_g - 10$ K equilibrium becomes inaccessible. In the following we will denote this temperature

range by the expression “WLF regime,” whether the considered liquids are molecular or polymeric ones. We will nevertheless specify whether the considered liquid is at equilibrium or in the process of ageing.

Another important feature of glass transition is the strongly heterogeneous nature of the dynamics close to T_g , which has been demonstrated experimentally over the past ten years^{9–28} using techniques such as NMR, fluorescence recovery after photobleaching translational and rotational probe diffusion, dielectric hole burning, or solvation dynamics. For reviews on this issue see, e.g., Refs. 29–31. These studies have demonstrated the coexistence of domains with relaxation time distributions spread over more than four decades at temperatures typically 20 K above T_g . An important feature is that the distribution widens when cooling the liquid.^{12,18} The characteristic size ξ of these domains, estimated by NMR,⁹ is typically 3–4 nm in the case of van der Waals liquids, whereas it can be as small as 1 nm in glycerol.¹¹ A model for the dynamics in the bulk has been proposed recently, which gives an interpretation for the heterogeneous dynamics in the bulk,^{32–34} in the case of van der Waals liquids. We proposed that the dynamics in the bulk is controlled by the percolation of slow domains corresponding to upward density fluctuations on the scale of a few nanometers. This model provides an expression for the characteristic size of the heterogeneities, expressed as a number of monomers N_c , as a function of temperature. N_c is found to be of order of a few hundreds at temperatures close to T_g and of order of a few tens at temperatures about 80 K above T_g .³³ Then, it provides an expression for the distribution of relaxation times in the WLF regime. Our model yields results that can be compared to the data obtained by Schmidt-Rohr and Spiess⁹ by NMR regarding the relaxation time distribution.

^{a)} Author to whom correspondence should be addressed.

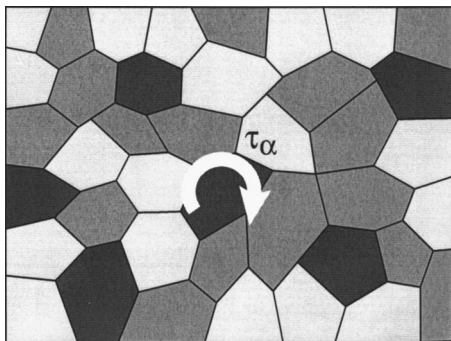


FIG. 1. The final relaxation mechanism in a van der Waals liquid, in the WLF (or VFT) regime. Dynamical subunits have been divided in three types: fast subunits (light gray), subunits of internal relaxation time τ_α (gray), and subunits with internal relaxation time $\tau \gg \tau_\alpha$ (dark gray). The ensemble of subunits with internal relaxation time larger or equal to τ_α percolates. The dominant relaxation time is τ_α , since the slowest subunits can rotate or diffuse in those with dominant time τ_α .

Our model allows also for explaining the violation of the Stokes law,^{12,18,33} which is related (1) to the increase of the width of the distribution and (2) to the increase of the dominant scale for dynamical heterogeneities when lowering the temperature. Another feature of our model is that it allows to interpret the shift of glass transition temperature measured in thin polymer films.^{35–41} Note that other authors have also considered this issue with different approaches.^{42,43} At this point, let us emphasize some essential differences between our model and that of Grest and Cohen,⁴⁴ in which percolation plays a role as well. In their model, the liquid is made of either fluid or truly rigid units. Glass transition corresponds to the percolation of these rigid units and appears thus to be a phase transition. In our model, the relaxation times of the subunits cover many decades but are finite: There is no phase transition. In a liquid in which the distribution of relaxation times covers many decades—which is the case over the whole WLF regime and, in particular, close to T_g —we argued that the dominant relaxation time in a mechanical experiment is that which corresponds to a percolation threshold as exemplified in Figs. 1 and 2. Other theoretical approaches, such as the Mode Coupling model, have been developed over the last decade (see, e.g., Ref. 45). This model deals with hydrodynamiclike equations for the density fluctuations and involves a nonlinear coupling with the density. This model predicts an arrest of the dynamics at a temperature T_{mc} above T_g and breaks down at molecular time scales of order of 10^{-9} s. It appears thus to be useful only at temperatures more than 80 K above the glass transition, as a consequence of its perturbative approach.⁴⁶ Numerical simulations are also used for studying liquid dynamics. For instance, some evidence that the dynamics is heterogeneous has been given using this technique.^{47,48} However, molecular dynamics simulations cannot be used for studying dynamics on time scales longer than 10^{-6} s or for studying equilibrium dynamics at temperatures below $T_g + 80$ K.

The aim of this paper is to propose an extension of this model which allows to describe ageing dynamics in van der Waals liquids and, in particular, to describe the role of dynamical heterogeneities in this process. Other models regarding ageing have been proposed.^{8,49–51} These models involve

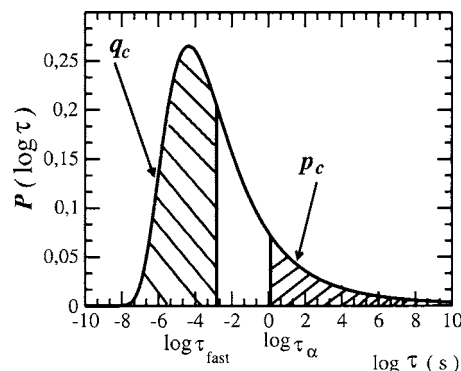


FIG. 2. Equilibrium relaxation time distribution at temperature T_g . τ_α is the relaxation time of dense subunits that percolate (fraction p_c) while τ_{fast} is the typical relaxation time of mobile units (fraction q_c). At equilibrium, one has $\tau_\alpha = \tau_{fast}^{N_c^{2/3}}$.

a set of coupled differential equations and allow for interpreting the evolution of macroscopic quantities, but the link to microscopic aspects was lacking. More recently, Diezemann has described some aspects of ageing process⁵² within the context of free energy landscape. Note, however, that there are no spatial aspects in neither of these previous models. Our aim here is precisely to propose a model which allows to calculate free energy barriers in van der Waals liquids and which allows to calculate their spatial distributions.

The model we develop is based on extensions of the so-called free volume models.³ At this stage one might raise the question whether it might be relevant, since it has been proven that the dynamics in liquids is not a function of the sole average density but of both the average density and of the temperature.^{53–61} The essential point is that the dynamics in the model we propose is not a function of the sole average density but *on the whole spectrum of density fluctuations*. At equilibrium, the latter is a function of both the average density ρ_{eq} and of the temperature T . Thus, intrinsically, the dynamics predicted by our model is a function of both parameters and is in principle compatible with experimental results described in Refs. 53–61.

The paper is organized as follows. First, in Sec. II A we summarized briefly our thermodynamical model for van der Waals liquids³² which allows to calculate statistical properties at equilibrium. Then, in Sec. II B and II C we summarize the basic ingredients of our model for the glass transition in van der Waals liquids.^{32–34} In particular, we discuss how we can determine the dominant scale of dynamical heterogeneities. We extend then our model to out-of-equilibrium situations. In Sec. II D we discuss which time scale is probed in a given experiment. In Sec. III we introduce our model for describing the ageing and rejuvenating dynamics. The results are discussed in Sec. IV. In particular, we discuss Kovacs memory experiment, the temporal asymmetry between ageing and rejuvenating, and the experiments of Ediger and co-workers on probe diffusion during ageing.

II. MODEL FOR THE GLASS TRANSITION IN van der WAALS LIQUIDS

In Secs. II A and II B, we introduce notations and definitions that will be used later in the text. Then we discuss

and specify some aspects of the model for the glass transition in the bulk that we proposed in Refs. 32–34 (Sec. II C), and we extend our model to out-of-equilibrium situations (Sec. II C).

A. Thermodynamical model for van der Waals liquids

Let us first recall briefly the thermodynamical model for polymer melts and van der Waals liquids proposed in Ref. 32. Expressions for the equilibrium density $\rho_{\text{eq}}(T)$, dimensionless thermal expansion coefficient χ_T , and bulk modulus K of the polymer melt were obtained as functions of the ratio T/T_c , where the temperature T_c is the only energy scale in the system and depends on the strength of van der Waals attractions between monomers (or molecules for a simple liquid). The density extrapolated down to $T=0$, which is analogous to a close packing density, is denoted by ρ_0 . The relevant temperature regime for the model presented here is $T \ll T_c$, which is well satisfied, since for usual polymers T_c is found to be of order 1000 K.³² Room temperature corresponds then to a low temperature regime, in which the correlation length of density fluctuations is comparable to the monomer length. In the low temperature limit, the following approximations are useful, even though not very accurate numerically:

$$\chi_T \sim \epsilon, \quad (1)$$

$$K \sim \frac{T\rho_0}{\epsilon^2} \approx \frac{T\rho_{\text{eq}}}{\epsilon^2}, \quad (2)$$

where the dimensionless quantity

$$\epsilon = \frac{\rho_0 - \rho_{\text{eq}}}{\rho_0} \quad (3)$$

can be interpreted as the free volume fraction. The parameters of the model are determined for each polymer by fitting the data regarding the bulk modulus and the density as a function of temperature.

B. WLF law

Here we introduce notations which allow us to write the standard WLF law in a form that we can use more readily later in the text. Throughout the paper, τ_α denotes the time which dominates the mechanical behavior of the liquid or melt. The variation of this relaxation time or of the viscosity in the bulk is given by the empirical WLF law (or VFT law in the context of simple liquids):^{3,62}

$$\log\left(\frac{\tau_\alpha}{\tau_\alpha(T_0)}\right) = \frac{-C_1(T-T_0)}{C_2+T-T_0}, \quad (4)$$

where T_0 is a temperature of reference, not to be confused with the Vogel temperature $T_\infty = T_0 - C_2$, which is sometimes also denoted by T_0 . Here, typically, T_0 is close to the glass transition temperature T_g , and $\tau_\alpha(T_0)$, the relaxation time at temperature T_0 , is a macroscopic time scale, e.g., comparable to 100 s. C_1 and C_2 are constants which depend on the considered polymers. One can see that the relaxation time is supposed to diverge at T_∞ . Typically, one has $T_\infty \sim T_g$

– 50 K. Note, however, that in practice, at temperatures below $T_g - 30$ K, the relaxation times become too long to be measurable, which means that Eq. (4) is in general checked at temperatures above $T_g - 20$ K or more. It was shown in Ref. 33 that Eq. (4) may be expressed in the equivalent form

$$\log \tau_\alpha = \log \tau_0 + \frac{\theta}{\tilde{\epsilon}}, \quad (5)$$

which depends explicitly on the density and is more readily useful for our glass transition model. θ is a number of order unity and τ_0 is a ballistic time of order 10^{-13} s. The quantity

$$\tilde{\epsilon} = \frac{\tilde{\rho}_0 - \rho_{\text{eq}}}{\rho_0} \quad (6)$$

is the “dynamical” free volume fraction. The density $\tilde{\rho}_0$ is smaller than ρ_0 , a fact which has been noted many years ago⁶² and for which we have no interpretation at this point.

The data regarding poly(vinyl acetate) (PVAc) that we will use in the following have been given in Ref. 33: $T_c = 1430$ K, $\rho_0 = 1.469$ g/cm³, and $\beta = 3.01$ (using data regarding thermodynamics of PVAc published in Ref. 63). The WLF parameters for PVAc are $T_0 = 311.1$ K, $C_1 = 15.57$, and $C_2 = 60$ K ($T_g = 310$ K, $M_w \sim 6.5 \times 10^5$ g/mol).^{62,64,65} With our notations, that corresponds to $\tilde{\rho}_0 = 1.2311$ g/cm³, $\theta = 0.536$, and $\log(\tau_\eta(T_0)/\tau_0) = 15.57$. Data regarding other liquids poly(methyl methacrylate) (PMMA), polystyrene (PS), poly(n-butyl methacrylate) (PBMA), polyisobutylene (PIB), and ortho-terphenyl (OTP) are given in Ref. 33.

C. Model for the glass transition in the bulk

In the model described in Refs. 32–34, we proposed that slow subunits correspond to upward density fluctuations and fast subunits to downward density fluctuations on a particular scale of $N_c = \rho V$. On a given scale, density fluctuations follow the Boltzmann law,

$$P(\delta\rho) \sim \exp(-\delta\rho^2 KV/2\rho_c^2 T). \quad (7)$$

By using the results of our thermodynamical model for van der Waals liquids, it is useful to define

$$\frac{\delta\rho}{\rho} = \frac{(\alpha - \alpha_\eta)\epsilon}{\sqrt{N_c}}. \quad (8)$$

α is a dimensionless quantity, which characterizes the amplitude of the considered fluctuations, and follows therefore the Gaussian statistics. The bare internal relaxation time of subunits corresponding to fluctuations α is then

$$\tau(\alpha) = \tau_0 \exp\left(\frac{\Theta}{\tilde{\epsilon} - (\alpha - \alpha_\eta)\epsilon/N_c^{1/2}}\right),$$

$$P(\alpha) = \frac{1}{(2\pi)^{1/2}} \exp\left(\frac{-\alpha^2}{2}\right), \quad (9)$$

with $\Theta = 2.3\theta$. Note that α_η is defined by

$$\int_{\alpha_\eta}^{\infty} P(\alpha) d\alpha = p_c, \quad (10)$$

where p_c is a three-dimensional percolation threshold, typically close to 0.1.³⁴ Note that the dominant relaxation time for the viscosity of the liquid is $\tau_\alpha = \tau(\alpha_\eta)$ as given by Eq. (9). The number $\alpha_\eta \sim 1$ is such that dimensionless density fluctuations larger than α_η (corresponding to relaxation times larger than τ_α) percolate. Thus in a mechanical experiment, one probes τ_α , while a wide distribution of relaxation times coexists in the system.³²⁻³⁴ These fluctuations have to be considered on a scale N_c of order a few hundreds of monomers. In Ref. 33 we proposed an expression for the scale N_c by considering two competing relaxation mechanisms: (1) the individual monomer jump time, which tends to increase sharply in subunits with large density fluctuations, and (2) the relaxation of density fluctuations, which is a collective process on the considered scale.

At this point, let us mention that one can distinguish two kinds of density fluctuations: long-lived density fluctuations, which can be associated with α relaxation, i.e., elementary monomer jumps, and short-lived ones associated with fast vibrations such as acoustic vibrations, which take place at fixed molecular environment.⁶⁷ The coexistence of density fluctuations associated with very different relaxation mechanisms can be inferred by considering, e.g., dilatational compliance measurements of liquids.⁶⁷ Liquids close to T_g exhibit a nonzero compliance $1/3K_0$ at time 0^+ , i.e., immediately after a hydrostatic stress is applied. Then, at long times, the dilatational compliance saturates to a higher value $1/3K$. The nonzero compliance at time $t=0^+$ can be associated with fast relaxation mechanisms of elementary time scale of order 1 ps, whereas the long time behavior is associated with the much longer α relaxation, i.e., the elementary monomer jumps. The latter are the relevant mechanisms that we consider in this paper. Therefore, following Robertson,⁶⁸ the density fluctuations that we consider in this paper are those associated with long relaxation processes, which are controlled by the compressibility $\delta_\kappa = 1/K - 1/K_0$. Indeed, the density fluctuations associated with the fast processes are not relevant for the heterogeneous nature of the dynamics. Note, however, that both moduli K and K_0 are comparable and that the ratio K/K_0 is of order of 0.3 typically. Therefore the approximation $\delta_\kappa \approx 1/K$ is numerically appropriate, particularly when considering other approximations made in the model for calculating the density fluctuation spectrum. Similarly, when heating or cooling a liquid, one can observe a short time thermal expansion coefficient α_g , smaller than the equilibrium one, α_l .⁶⁷ The thermal expansion coefficients α_g and α_l are associated with the same degrees of freedom as K_0 and K , respectively.

We discuss the determination of N_c now.

1. Scale of dynamical heterogeneities

Let us now derive N_c from this model. The issue is to determine which processes lead to the longest dominant relaxation time in liquids in the WLF regime. We are primarily concerned here by relaxation processes which control the

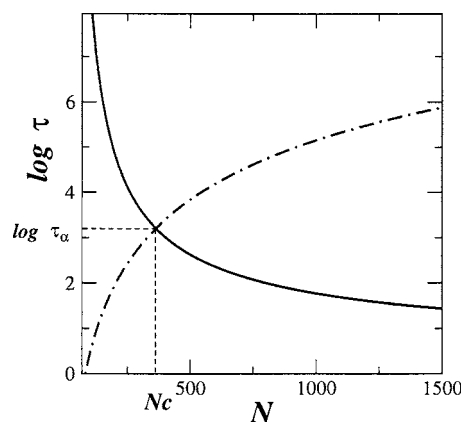


FIG. 3. Determination of the length scale of dynamical heterogeneities. The black solid line represents the relaxation time τ_j^+ given by Eq. (12) and $\alpha^- < 0$ while the dashed-dotted line represents the lifetime of density fluctuations τ_{life} [see Eq. (13)]. On large scale, density fluctuations are long lived. On shorter length scales, one observes comparatively large density fluctuations, which should lead to large relaxation times τ_j . On the other hand, on short length scales, density fluctuations are short lived. There exists an intermediate length scale on which one has large density fluctuations which are long lived. That corresponds to the scale of dynamical heterogeneities N_c .

viscosity of the system. As described above, the longest relaxation times will take place in subunits with large density fluctuations. The WLF law corresponds to the relaxation time of these slow subunits. It means that $\tilde{\rho}_0$ takes the large density fluctuations into account. Therefore the monomer jump time

$$\tau_j = \tau_0 \exp\left(\frac{\Theta}{\tilde{\epsilon}}\right) = \tau_\alpha \quad (11)$$

corresponds to monomers in dense subunits. On scale N , typical free volume fluctuations are of order of $\alpha\epsilon/N^{1/2}$, where α is a number of order of 1. Therefore, monomers with jump time given by Eq. (11) coexist with monomers with jump time given by

$$\tau_j^\pm = \tau_0 \exp\left(\frac{\Theta}{\tilde{\epsilon} + \alpha^\pm \epsilon/N^{1/2}}\right), \quad (12)$$

which can be either much smaller (τ_j^- , with $\alpha^\pm = \alpha^+ > 0$) or much larger (τ_j^+ , with $\alpha^\pm = \alpha^- < 0$) than τ_α . Equation (12) means that by considering small scales, one can find monomers with very large monomer jump time ($\alpha^\pm \sim -1$) as given by the free volume model, with probability of order of 1 (see Fig. 3). The time τ_j^+ would be the monomer jump time if the density was maintained fixed by imaginary wall. On the other hand, the density of the subunit has a finite lifetime. For τ_j^+ to be the effective monomer jump time, the environment of the monomer—i.e., the density of the subunit—has to be kept at a large density during a time interval of at least τ_j^+ : The lifetime of the considered density fluctuation has to be at least τ_j^+ (see in Fig. 3).

Let us now consider the lifetime τ_{life} of density fluctuations on the scale of N monomers. The corresponding length scale is thus $\xi = aN^{1/3}$, where a is one monomer length. We consider positive density fluctuations with large bare monomer jump time. Such a subunit is surrounded by other sub-

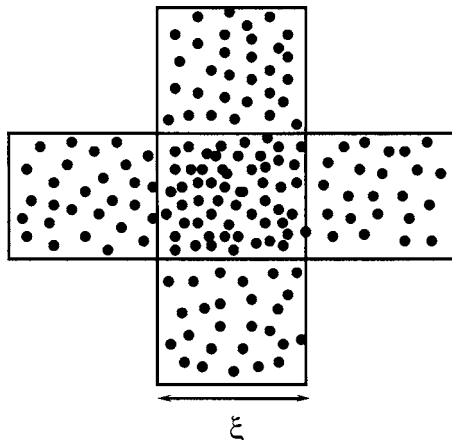


FIG. 4. Two mechanisms compete for determining the α relaxation: (1) local reorganization of free volume, at fixed local density, and (2) diffusion of the densest subunit in the more mobile neighboring subunits. A dense subunit can be melted by its mobile neighbors. A subunit of large density will melt and relax in a longer time if it is surrounded only by subunits that are themselves relatively slow. The lifetime of a dense subunit surrounded by much faster subunits with internal relaxation time τ_{fast} is $\tau_{\text{life}} = \tau_{\text{fast}} N^{2/3}$. This time is frequently shorter than the relaxation time a dense subunit would have if its overall density was maintained fixed by imaginary walls. The latter would be τ_j^+ as given in the text by Eq. (12) with $\alpha < 0$.

units corresponding to various density fluctuations, some of them corresponding to lower density fluctuations. Then, the dense subunits we consider will dissolve in the surrounding subunits of lower density by a diffusion process as one can see in Fig. 4. This diffusion process occurs at the boundary of the considered subunit, and the monomer time jump is that of the lower density neighboring subunits in which it diffuses. Since the lifetime of density fluctuations is controlled by a diffusion process, this lifetime is proportional to the scale $\xi^2 \propto N^{2/3}$ that we consider. Indeed, we assume that density fluctuations on scale of q^{-1} relax with the usual diffusion laws, i.e., $\tau(q) \propto q^{-2} \tau_{\text{fast}}$, where τ_{fast} is the local monomer jump time in the rapid neighboring subunit as given by Eq. (12) with $\alpha \sim 1$ (see in Fig. 4). Therefore the lifetime of a considered density fluctuation on the scale N is then

$$\tau_{\text{life}} \sim \tau_0 N^{2/3} \exp\left(\frac{\Theta}{\bar{\epsilon} + \alpha \epsilon / N^{1/2}}\right), \quad (13)$$

where α is of order of 1, since the diffusion will take place primarily through the most rapid environment with non-negligible probability. Then, the larger the scale, the longer the lifetime of density fluctuations as one can see in Fig. 3.

In summary here, we deduce from the preceding discussions that by considering small enough scales, one can find, with probability of order of 1, very dense subunits. The relaxation time of these subunits should be therefore very long [given by Eq. (12) with $\alpha < 0$]. However, another relaxation process competes with the individual monomer jumps and corresponds to the relaxation of density fluctuations. At small scale, this process is faster than the individual monomer jump time one would observe if the density was maintained fixed. At small scale it is therefore the dominant relaxation time (see Figs. 3 and 4). Therefore the largest relaxation times in the system are determined by the relation

$$\tau_{\text{life}} = \tau_j^+, \quad (14)$$

which yields

$$N_c \approx \frac{\Theta^2 \epsilon^2}{\bar{\epsilon}^4} \frac{1}{(\ln(\Theta^2 \epsilon^2 / \bar{\epsilon}^4))^2}. \quad (15)$$

The scale $\xi = a N_c^{1/3}$ (a is one monomer length) is thereby the smallest scale at which the density fluctuation lifetime is equal or larger than τ_α . Density fluctuations on smaller scales are irrelevant being too short lived. Assuming that the WLF law [Eq. (5)] may be used on the scale N_c and using Eqs. (1) and (2), the relaxation time distribution may be written as in Eq. (9), on the scale N_c given by Eq. (15). The main feature of the scale N_c is that it is of order of a few hundreds typically close to T_g and that it decreases when increasing the temperature.³³

2. Equilibrium and out-of-equilibrium situations

We represented in Fig. 2 the distribution of relaxation time when the sample is at equilibrium. By definition then, one has the relation

$$\tau_\alpha = \tau_{p_c} = N_c^{2/3} \tau_{\text{fast}}, \quad (16)$$

where τ_{p_c} is defined by

$$\int_{\tau_{p_c}}^{\infty} P(\tau) d\tau = p_c, \quad (17)$$

where $P(\tau)$ here is the equilibrium distribution of relaxation times. The time τ_{fast} is the local relaxation time of fast neighboring subunits and corresponds to the q_c -fastest subunits:

$$\int_0^{\tau_{\text{fast}}} P(\tau) d\tau = q_c. \quad (18)$$

q_c is to be determined. We will see below that q_c can be taken to be 30%. There is indeed two cutoffs at long times in the bare distribution of relaxation times. One corresponds to the 10% or so slowest and corresponds to the percolation threshold. Another corresponds to the melting process due to the faster subunits. By definition, at equilibrium, both times are equal as written in Eq. (16). In out-of-equilibrium situations, one can consider two different cases: (1) one which corresponds to a distribution which is wider than that at equilibrium (see Fig. 5 and 2) another one which corresponds to a distribution which is narrower than that at equilibrium as one can see in Fig. 6. One will see below that case (1) corresponds to the situation in which one heats a sample up, whereas the second one corresponds to the situation in which one cools a sample and let it age. In both cases, the dominant relaxation τ_α is given by a cutoff in the distribution. In case (1), the cutoff corresponds to the time

$$\tau_\alpha = N_c^{2/3} \tau_{\text{fast}} < \tau_{p_c}, \quad (19)$$

which is smaller than the time corresponding to the percolation threshold. The times τ_{fast} and τ_{p_c} are still defined by Eqs. (18) and (17), but here $P(\tau)$ is a time dependent out-of-equilibrium distribution of relaxation times. In case (2), the cutoff is given by the percolation requirement

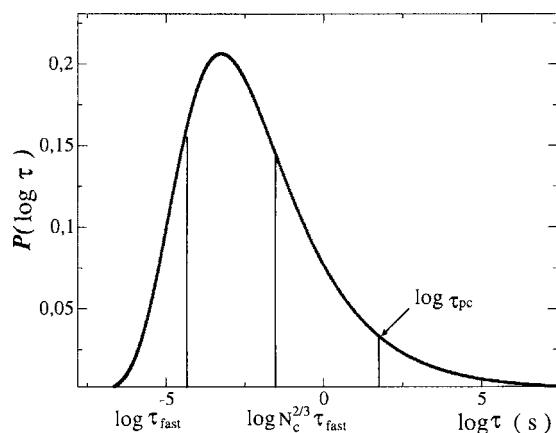


FIG. 5. When the distribution of internal relaxation times is broader than that at equilibrium, the dominant relaxation time, that is, the effective cutoff in the distribution, is given by $\tau_\alpha = N_c^{2/3} \tau_{\text{fast}}$ which is then smaller than τ_{pc} .

$$\tau_\alpha = \tau_{pc} < N_c^{2/3} \tau_{\text{fast}}. \quad (20)$$

Again, τ_{fast} and τ_{pc} here are also defined by Eqs. (18) and (17), with $P(\tau)$ here is a narrow out-of-equilibrium distribution of relaxation times. Thus, in the general situation, the dominant relaxation time is given by

$$\tau_\alpha = \min[N_c^{2/3} \tau_{\text{fast}}, \tau_{pc}]. \quad (21)$$

Only in the equilibrium conditions are the two times of the left hand side of this equation equal.

3. What is α relaxation

The preceding discussions are essential for defining what the α relaxation is from a microscopic point of view. The α relaxation corresponds to some molecular jumps, but not all molecular jumps contribute or correspond to the α relaxation. Only the molecular jumps of the 10% slowest molecules or monomers do contribute to the α relaxation. Other jumps, occurring on shorter time scales, correspond only to individual diffusion and do not contribute to, e.g., stress relaxation in macroscopic experiments. For instance, following individual molecules in, e.g., a numerical simulations will give information on the molecule diffusion. On the other hand, a very small fraction of the individual jumps will contribute to α relaxation. If we assume a four decade wide relaxation time distribution, the 10% slowest particles will contribute to only a fraction of 10^{-5} of the overall monitored individual jumps. Moreover identifying them is certainly not straightforward. Therefore, following individual molecular jumps in numerical simulations⁴⁸ or in the case of colloidal systems⁶⁶ does not provide insight to α -relaxation mechanisms, unless a proper and experimentally time consuming analysis is performed. The latter requires to have a clear understanding of what α relaxation is.

4. How α relaxation occurs

From the preceding discussion, we see that two processes compete for allowing individual molecular jumps. (1) One corresponds to a jump at fixed local free volume. By that, we mean that there is no reallocation of free volume on

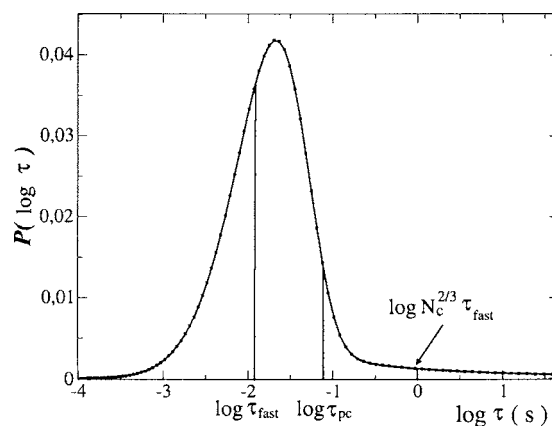


FIG. 6. When the distribution of internal relaxation times is narrower than that at equilibrium, the dominant relaxation time, that is, the effective cutoff in the distribution, is given by $\tau_\alpha = \tau_{pc}$ which is then smaller than $N_c^{2/3} \tau_{\text{fast}}$.

a scale larger than $aN_c^{1/3}$ on the considered time scale. This is the dominant process in relatively fast subunits, because there is a large amount of local free volume. This is therefore the dominant process in molecular diffusion. (2) The second one is the dominant one in relatively slow subunits. The local fraction of free volume is too small for allowing a molecular jump at fixed local fraction of free volume. Local reorganization of the free volume would be too slow for allowing an individual molecular jump on the corresponding time scale. The process of dissolution by diffusion in faster neighboring subunits is much faster. Then, once the local fraction of free volume has increased, an individual molecule can jump. This process happens in a time that is smaller than the time which would be required if the initial density was maintained fixed by imaginary walls. (3) The α -relaxation time corresponds to the melting time of relatively dense subunits by neighboring faster subunits.

D. Interpretation of the model

Equation (9) provides the distribution of internal relaxation times of subunits. An example of such distributions is displayed in Fig. 2. The basic idea of our model is that in a mechanical experiment, the dynamics is controlled by the time associated with the percolation threshold as defined by Eq. (10). It is important to emphasize at this point that the corresponding time $\tau_\alpha = \tau(\alpha_\eta)$ corresponds to an effective long time cutoff in the relaxation time distribution: A subunit of very large internal relaxation time $\tau \gg \tau_\alpha$ (as given by the tail of the distribution) is on average surrounded by faster subunits of dominant relaxation time τ_α . In a shear experiment, these slow subunits reorient as a whole with the characteristic time τ_α itself. In a dilatational experiment, they may move away from the constraint path on time scale τ_α also so as to allow the contraction of the liquid. In many experiments, the longest relevant relaxation time that is measured is therefore τ_α even though subunits with much longer internal relaxation time exist in the liquid (see Fig. 1). However, because the distribution of relaxation times is wide and since we argue that it corresponds to spatial heterogeneities, one must ask whether different techniques measure, or not, the same relaxation time.

1. Small probe diffusion

Note first that the issue of the time probed by a given technique versus the time probed by another one is relevant. Ediger and co-workers^{12,13,16} and Fujara *et al.*¹⁸ for instance have shown that the variation with temperature of the time scale associated with probe diffusion is different from that of the dominant time measured in mechanical or dielectric spectroscopy and that the corresponding discrepancy can increase up to three orders of magnitude when lowering the temperature. However, there is a fundamental difference between the diffusion coefficient of a probe molecule and the dominant relaxation time in, e.g., mechanical or dielectric experiments. Indeed, the diffusion coefficient depends on the relaxation time distribution $P(\tau)$ [Eq. (9)] by a relation of the type

$$D \sim \int_{\tau_{\text{fast}}}^{\infty} \frac{1}{\tau} P(\tau) d\tau \approx \tau_{\text{fast}}^{-1} \quad (22)$$

and is therefore dominated by the fastest relevant time τ_{fast} available to the probe in the system³³ (see Fig. 2). It is a short time cutoff in Eq. (22), which depends on the relative size of the probe and of the scale ξ of the heterogeneities.³³ When the scale of the heterogeneities is smaller than the size of the probe $\tau_{\text{fast}} \approx \tau_{\alpha}$. In the lower temperature regime, the scale of heterogeneities might become larger than the probe diameter, and τ_{fast} becomes smaller than τ_{α} . The discrepancy then increases when lowering the temperature, up to several orders of magnitudes, depending on the system.^{12,18,33} On the other hand, let us note that in the same experiments as those performed by Ediger and co-workers,^{12,13,16} quantities which are dominated by the longest relevant times, such as the integrated time correlation function of the probe orientation, provide the same dominant time scale as that measured by dielectric spectroscopy or mechanical spectroscopy.

2. Measuring τ_{α} in mechanical experiments

A dominant relaxation time in a supercooled liquid can be measured using a great diversity of techniques. For instance, one can measure the relaxation of the deformation after an instantaneous and small variation of pressure or after a small shear stress is applied. This time can be measured experimentally as a peak at low frequency of the imaginary part of $J_2^*(\omega, T)$ or of $J_1^*(\omega, T)$, where $J_2(t, T)$ and $J_1(t, T)$ are the time dependent dilatational compliance and the transient shear compliance of the liquid, respectively.⁶⁷ $J_2^*(\omega, T)$ and $J_1^*(\omega, T)$ are the corresponding compliances in frequency. One can, e.g., look at $J^*(\omega, T)$ at fixed temperature, as a function of frequency. Then, the α relaxation corresponds to the peak at low frequency. When the corresponding peak is located at $\omega \sim 10^{-2}$ s, the temperature is the glass transition temperature. The corresponding relaxation in this frequency regime can be studied, e.g., by dilatometry. Mechanical⁶⁹ or photon correlation spectroscopy^{70,71} can be used over a wider frequency range and allows for a measurement of $J_2(t, T)$. The dominant relaxation time can be alternatively determined as the integrated value of the time correlation function:

$$\tau_{\alpha} = \int_0^{\infty} F(t) dt \approx \int_0^{\tau_{\text{cutoff}}} \tau P(\tau) d\tau \approx \tau_{\text{cutoff}}, \quad (23)$$

where $F(t)$ might be $J_1(t, T)$, $J_2(t, T)$, or, e.g., the low- q structure factor $S(q, t)$. Note that Eq. (23) is very different from Eq. (22) and might yield different dominant time scales indeed. Since the relaxation time distribution (Fig. 2) is almost flat when plotted as a function of time scale τ (and not as a function of $\log \tau$), the time in Eq. (23) is essentially equal to the cutoff at long times in the relaxation time distribution, as defined by Eq. (10). Thus we do not make any distinction between the effective cutoff in the relaxation time distribution τ_{cutoff} and the dominant relaxation time τ_{α} .

III. AGEING DYNAMICS

When cooling below T_g , various quantities evolve with time. The volume of the sample decreases with time, with a decreasing but never vanishing rate.⁵⁻⁸ The compliance also evolves with the ageing time t_w .⁴ Struik proposed the following relation:

$$J(t, t_w) = \mathcal{J}\left(\frac{t}{t_w^{\mu}}\right), \quad (24)$$

where μ is close to 1 at temperature a few tens of Kelvins below T_g . The enthalpy of samples also evolves slowly with time during ageing.^{72,73} Recently, some authors have considered ageing from a microscopic point of view. Thureau and Ediger^{21,23} and Sasaki *et al.*²² measured the orientation correlation time of small probes in ageing liquids and found a relation $\tau_c \propto t_w^{\mu}$ with $\mu \approx 0.2$. The fact that this exponent is small can be attributed to the shallow temperature quench at only $T_g - 5$ K. Though ageing involves huge time scales, its effect can be erased on a much shorter time scale, which can be called temporal asymmetry. It has been shown, in particular, by Kovacs.⁷ After ageing for a few thousand hours, the system is rejuvenated by heating in a much shorter time scale. Another effect, also described by Kovacs and other authors, is the so-called Kovacs memory effect.⁷⁴⁻⁷⁷ The experiment is the following: Let us consider a system cooled at a temperature well below T_g , which is then allowed to age. Then, if it is reheated, the evolution of the volume can be nonmonotonous and exhibits an overshoot for particular ageing times and reheating temperatures. The amplitude of the effect can be of order of 0.1%.

When cooling a liquid at temperatures not too far below T_g , the thermodynamical state of the system becomes stationary within an accessible experimental time. We assume then that the system is at thermodynamical equilibrium, since all physical quantities can be extrapolated from equilibrium data above T_g .^{72,78} At lower temperatures, we assume that ageing corresponds to the relaxation towards equilibrium, even though this equilibrium cannot be reached in experimentally accessible times. Out of equilibrium, i.e., before the system has had time to equilibrate, let us introduce the out-of-equilibrium excess free energy:^{79,80}

$$F = \int p(\rho) \ln\left(\frac{p}{p_{\text{eq}}}(\rho)\right) d\rho, \quad (25)$$

where $p_{\text{eq}}(\rho)$ is the equilibrium density fluctuation distribution on the scale N_c . The time derivative of the excess free energy is given by

$$\frac{dF}{dt} = \int \frac{\partial p}{\partial t} \ln\left(\frac{p}{p_{\text{eq}}}(\rho)\right) d\rho, \quad (26)$$

which we can be written in the form

$$\frac{dF}{dt} = \int J \frac{\partial}{\partial \rho} \ln\left(\frac{p}{p_{\text{eq}}}(\rho)\right) d\rho. \quad (27)$$

The latter is the continuous equivalent of the standard Onsager equation,⁸⁰

$$\frac{dF}{dt} = \sum_i J_i F_i, \quad (28)$$

where J_i is a flux and F_i a thermodynamical force. Here the thermodynamical force which drives the system towards equilibrium is $(\partial/\partial_p) \ln(p/p_{\text{eq}})$. In the linear regime of out-of-equilibrium statistical mechanics, one has a linear relation between the flux and the forces of the form

$$J_i = L_{ij} F_j \quad (29)$$

where L_{ij} is an Onsager matrix coefficient. Here summation over repeated indices is implicit. We thus assume a linear relation between the flux J and the force $(\partial/\partial_p) \ln(p/p_{\text{eq}})$ of the form

$$J(\rho) = - \int L(\rho, \rho') \frac{\partial}{\partial \rho'} \ln\left(\frac{p}{p_{\text{eq}}}(\rho')\right) d\rho'. \quad (30)$$

We make the additional assumption that the previous relation is local in density space, which means that L is diagonal. One has then

$$J(\rho) = - L(\rho) \frac{\partial}{\partial \rho} \ln\left(\frac{p}{p_{\text{eq}}}(\rho)\right). \quad (31)$$

Conservation of probability implies

$$\frac{\partial p}{\partial t} + \frac{\partial J}{\partial \rho} = 0. \quad (32)$$

We thus obtain

$$\frac{\partial p}{\partial t} - \frac{\partial}{\partial \rho} \left(\gamma(\rho) p_{\text{eq}}(\rho) \frac{\partial}{\partial \rho} \left(\frac{p}{p_{\text{eq}}}(\rho) \right) \right) = 0, \quad (33)$$

which is a Fokker-Planck equation, where $\gamma(\rho)$ is a diffusion coefficient in density space. By definition one has $L(\rho) = \gamma(\rho) p_{\text{eq}}$. The value assumed by $\gamma(\rho)$ depends not only on ρ here but on the whole density distribution $p(\rho)$. Therefore we denote the transition rate by $\gamma(\{\rho\})$ in the following. According to the discussions in the previous sections, τ_α is the longest relevant relaxation time and is given by

$$\tau_\alpha(t) = \min[N_c^{1/2} \tau_{\text{fast}}, \tau_{p_c}], \quad (34)$$

where τ_{p_c} corresponds to the relaxation time of subunits with densities such that

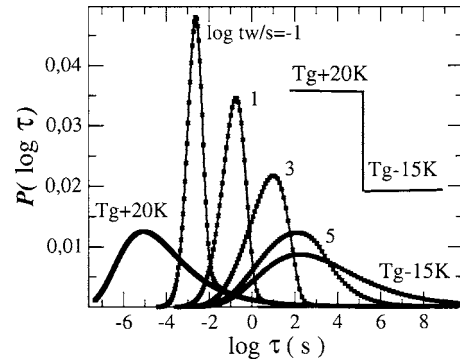


FIG. 7. Relaxation time distributions, as a function of time, calculated solving the Fokker-Planck equation (33) for PVAc. The polymer has been cooled from $T_g + 20$ K to $T_g - 15$ K at time 0. The waiting times are $\log t_w$ (s) = -1, 1, 3, and 5. We plotted also both equilibrium distributions at $T_g + 20$ K and $T_g - 15$ K.

$$\int_{\tau_{p_c}}^{+\infty} P(\tau) d\tau = p_c, \quad (35)$$

where p_c is a percolation threshold that is taken to be 0.08.³⁴ $P(\tau)$ is the distribution of relaxation times calculated as

$$\pi(\alpha) = \tau_0 \exp\left(\frac{\Theta}{\tilde{\epsilon} + (\alpha_\eta - \alpha)\epsilon/\sqrt{N_c}}\right), \quad (36)$$

$$\alpha(\rho) = \frac{\sqrt{N_c}}{\epsilon} \left(\frac{\rho - \rho_{\text{eq}}}{\rho} \right). \quad (37)$$

ρ_{eq} is the equilibrium density fluctuation at temperature T . The relaxation time τ_{fast} is calculated as

$$\int_0^{\tau_{\text{fast}}} P(\tau) d\tau = q_c, \quad (38)$$

where q_c will be an adjustable parameter that we will adjust on some experimental data, which is a few tens of percent. This relaxation time determines the lifetime of density fluctuations. The spectrum of relaxation times $\gamma^{-1}(\{\rho\})$ is determined as follows:

$$\gamma(\{\rho\}) \sim \begin{cases} \tau^{-1} & \text{when } \tau < \tau_\alpha(t) \\ \sim \tau_\alpha^{-1}(t) & \text{otherwise.} \end{cases} \quad (39)$$

IV. RESULTS AND DISCUSSION

Here we present and discuss the results of our numerical simulations. To this end the Fokker-Planck equation (33) is solved by discretizing the density phase space (see Appendix). Let us first consider the case of temperature down jump and let us consider the evolution of the relaxation time distribution. In Fig. 7, we plotted the distribution of relaxation time of PVAc when the temperature is cooled from $T_g + 20$ K to $T_g - 15$ K. The distribution is plotted at various intermediate times t_w . We plotted both equilibrium distributions at $T_g + 20$ K and at $T_g - 15$ K. We note that the distribution translates towards longer times as the system ages. We observe also that the distribution is slowed by the longest relaxation time $\tau_\alpha(t)$ and that the latter controls the overall evolution of the relaxation time distribution. Here, the situa-

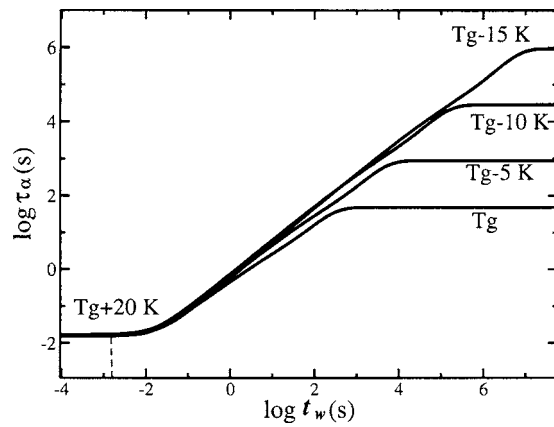


FIG. 8. Dominant relaxation time $\tau_\alpha(t_w)$ in PVAc as given by Eq. (34) during temperature down jumps at temperatures below T_g : $T_g - 15$ K, $T_g - 10$ K, $T_g - 5$ K, and T_g . The initial temperature is $T_g + 20$ K. In the ageing regime, the dominant relaxation time $\tau_\alpha(t)$ is proportional to t_w^μ with $\mu \approx 1.0$ here.

tion is that of case (1), for which the distribution of relaxation times is narrower than that at equilibrium. The dominant relaxation time $\tau_\alpha(t)$ is equal to τ_{p_c} , whereas the melting time $\tau_{\text{fast}} N_c^{2/3}$ would be larger than τ_{p_c} . At an ageing time t_w , the dominant relaxation time is comparable to t_w . Note that the dominant relaxation time at the equilibrium state at $T_g - 10$ K which is comparable to 10^6 s indicates that we would need to age for a few weeks to reach this equilibrium distribution. We consider now the evolution of the dominant relaxation time $\tau_\alpha(t)$. As we discussed, here one has

$$\tau_\alpha(t) = \tau_{p_c}, \quad (40)$$

where τ_{p_c} is defined by Eq. (35). The evolution of $\tau_\alpha(t)$ for temperature down jumps from $T_g + 20$ K down to various temperatures is plotted in Fig. 8. In a first step, the dominant relaxation time is equal to that of the initial temperature,

$$\tau_\alpha(t_w) = \tau_\alpha(T_i) \quad \text{for } t_w < \tau_\alpha(T_i). \quad (41)$$

Then, after an elapsed time comparable to the latter, it starts increasing with an exponent close to 1, up to the equilibrium value at the final temperature. After a time $t_w > \tau_\alpha(T_i)$:

$$\tau_\alpha(t_w) = C t_w^\mu \quad \text{for } \tau_\alpha(T_i) < t_w < \tau_\alpha(T_f). \quad (42)$$

Here μ is close to 1.0: The relaxation time evolves proportionally with the elapsed time t_w . This regime lasts until a waiting time t_f comparable to $\tau_\alpha(T_f)$, where $T_f = T_g - 15$ K here. At longer times one has

$$\tau_\alpha(t_w) = \tau_\alpha(T_f) \quad \text{for } t_w > \tau_\alpha(T_f). \quad (43)$$

Other temperature down jumps have also been plotted in Fig. 8. At long times, one has $\tau_\alpha \propto t_w^\mu$ for which the exponent does not depend very much on the final temperatures, for all these deep down jumps. For weaker down jumps (not shown) one observes that the ageing exponent is smaller and decreases here down to $\mu \approx 0.4$ for the 3 K down jump. Note that this is consistent with results by Struik⁴ and by Thureau and Ediger.²³ These last authors have measured the evolution of the rotational correlation time τ_c of small probes. For a 5 K down jump, they observed an ageing exponent of 0.2.

A. Influence of the initial temperature

We can calculate the evolution of the dominant relaxation time as given by Eq. (34) for various temperature up jumps. The ageing exponent does not depend on the initial temperature and is close to 1. The corresponding relaxation time distribution has been plotted in Fig. 9. The volume as a function of time is given by

$$v(t_w) = \int \frac{p(\rho, \tau_w)}{\rho} d\rho. \quad (44)$$

For calculating the evolution of the volume, one needs to know the respective values of α_g and α_l . For instance, after a change of temperature ΔT at time 0, we assume that there is an instantaneous variation of the volume at time 0^+ of amplitude $\alpha_g \Delta T$, followed by a slow evolution of the volume towards equilibrium of amplitude $(\alpha_l - \alpha_g) \Delta T$. In the case of PVAc we take $\alpha_l \approx 6 \times 10^{-4} \text{ K}^{-1}$ and $\alpha_g \approx 2 \times 10^{-4} \text{ K}^{-1}$.⁶² Therefore, the Fokker-Planck equation (33) must be understood as describing the evolution of the slow degrees of freedom and not that associated with fast vibrations (phonons). Regarding this slow component of the evolution of the volume, we observe here also two regimes. In a first step, the volume is equal to that just after the very fast degrees of freedom have adjusted at time 0^+ (α_g contribution). This process lasts for a time t_i which is small as compared to the dominant relaxation time at the initial temperature: This is due to the contribution of the fast part of the relaxation time spectrum (see, e.g., in Fig. 2). In particular, at a time $t_w < \tau_\alpha(T_i)$, the volume can have significantly decreased. In a second step, the volume decreases linearly with the logarithm of the waiting time t_w . One has

$$\frac{dv}{d \log t_w} = -\lambda \quad \text{for } t_i \leq t_w \leq t_f = \tau_\alpha(T_f). \quad (45)$$

The logarithmic decrease of the volume is well documented experimentally.^{5,72,75,76,78} Finally, the system reaches equilibrium after a time comparable to $\tau_\alpha(T_f)$,

$$v(t_w) = v_{\text{eq}}(T_f) \quad \text{for } t > t_f. \quad (46)$$

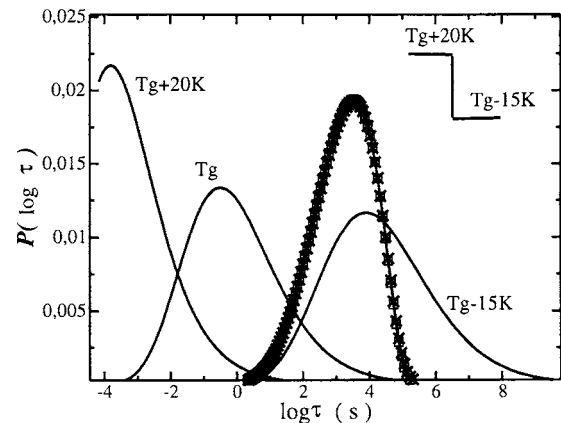


FIG. 9. Distribution of relaxation times in PVAc after an aging time $t_w = 10^5$ s at $T_g - 15$ K. The initial temperatures are T_g (\square) and $T_g + 20$ K (\times), respectively. There is no measurable difference between both distributions at the considered aging time, provided the latter is larger than any relevant time scale of the initial distributions.

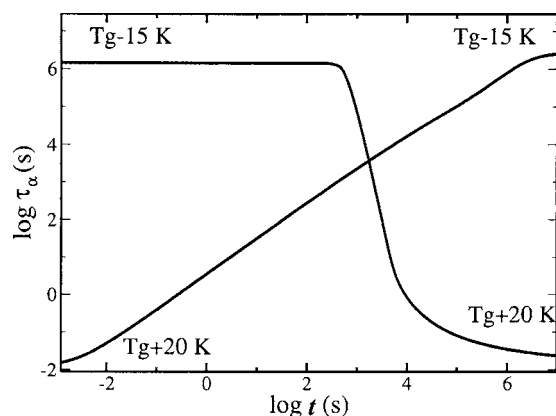


FIG. 10. Dominant relaxation time of PVAc, during a temperature down jump between T_g+20 K and T_g-15 K and during a temperature up jump at T_g+20 K of a polymer sample initially at equilibrium at T_g-15 K. These curves are calculated using the Fokker-Planck equation without coupling for the dynamics between dense subunits and mobile subunits ($q_c=1.0$). The time scale which controls both evolutions is the same and is the dominant equilibrium relaxation time $\tau_\alpha(T)$ at the lowest temperature $T=T_g-15$ K.

B. Reheating and temporal asymmetry

We study here the time it takes for the system to reach back equilibrium, after it is heated from a temperature below T_g up to a temperature above T_g . We show here that dynamical heterogeneities are key for understanding temporal asymmetry. First we solve the Fokker-Planck equation (33) without coupling between the dynamics of dense and less dense subunits. Technically, it amounts to take $q_c=1.0$. In this way, the longest relaxation time is always equal to τ_{p_c} defined by Eq. (35). We denote this by the Fokker-Planck equation without coupling.

1. Fokker-Planck equation without dynamic coupling between dense and fast subunits

In Fig. 10, we plotted the evolution of the dominant relaxation time τ_α after a temperature up jump from T_g-15 K up to T_g+20 K. In a first time, the dominant relaxation time is stationary and equal to that at the initial temperature. In this regime the dynamics is slow. After an elapsed time of about $t \approx 10^3$ s, the dominant relaxation time decreases with time. In a first step, the decrease is rapid, and then the variation slows down. Finally, the dominant relaxation time becomes equal to that at equilibrium at the final temperature. This process takes a time which is comparable to the dominant relaxation time at the initial temperature: This is a very long process, and there is no temporal asymmetry. In the same conditions, the volume relaxes very slowly towards the equilibrium value. At short times (i.e., t_w smaller than 1 s), the volume is stationary. At longer times, the volume increases and reaches equilibrium on a time scale comparable to the initial dominant relaxation time $\tau_\alpha(T_i)$. This is not what is observed experimentally. Indeed, the time to reach equilibrium when heating a sample is much smaller than the initial dominant relaxation time. The problem of the present model can be observed in Fig. 11 in which we plotted the evolution of the relaxation time distribution. We see here that even at long heating times, there remain long relaxation times in the system. The latter disappear after a time $\tau_\alpha(T_i)$.

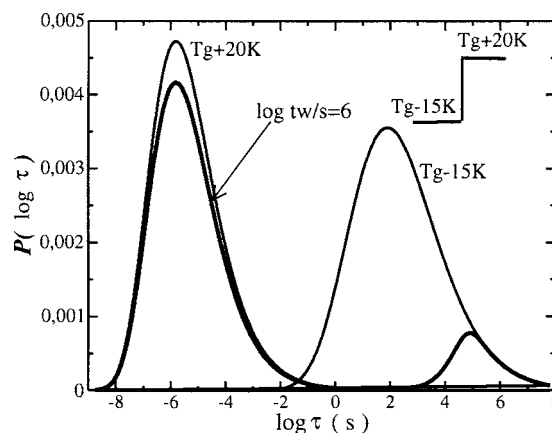


FIG. 11. Distribution of relaxation times during a temperature up jump at T_g+20 K of a polymer sample initially at equilibrium at T_g-15 K. The evolution is calculated using the Fokker-Planck equation without coupling ($q_c=1.0$). We see that long relaxation times persist a long time ($t=10^6$ s) after the temperature has been increased. This persistence explains the absence of temporal asymmetry observed in the absence of coupling. We have displayed also the initial distribution of relaxation times (equilibrium at T_g-15 K) and the final one (equilibrium at T_g+20 K).

2. Fokker-Planck equation with dynamical coupling between fast subunits and dense subunits

Thus, we deduce that the temporal asymmetry is the consequence of the dynamical coupling between fast and slow subunits. Indeed, when heating a sample, fast subunits become faster in a comparably short time scale. Then, they are able to melt dense/slow subunits in a time that is much shorter than the α -relaxation time at the initial temperature T_i . Here we solve the Fokker-Planck equation by taking into account this dynamic coupling. This coupling is determined by the value of the parameter q_c [see Eq. (38)]. To determine the correct value of this parameter, we consider the evolution of the volume as a function of time during a heating process, with various values of q_c , and confront the resulting dynamics to experimental data. In Fig. 12 we plotted the evolution of the volume after heating a sample for three different values of q_c : 20%, 30%, and 40%. The evolution which is the

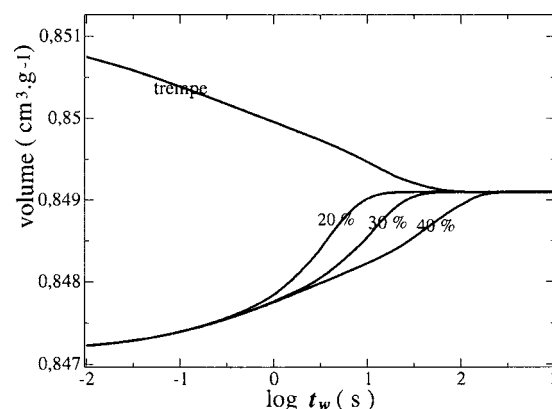


FIG. 12. Volume during a temperature down jump from T_g+5 K down to T_g and during a temperature up jump from T_g-5 K to T_g calculated using Eq. (44). The different temperature up jump curves correspond to different choices of the parameter q_c [see Eq. (34)]. From left to right: $q_c=20\%$, 30% , and 40% . The larger the value of q_c , the longer it takes for melting slow subunits. We found the value of $q_c=30\%$ to provide reasonable agreement with known experimental melting time scales (Ref. 5).

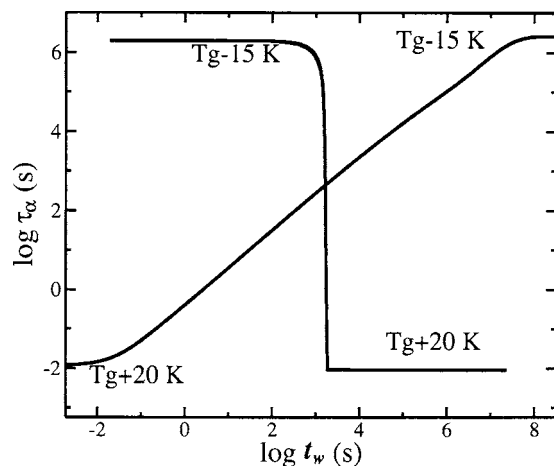


FIG. 13. We compare here the evolution of the dominant relaxation time during a temperature down jump between T_g+20 K and T_g-15 K and during a temperature up jump between the same temperatures. The dominant relaxation time is calculated solving the Fokker-Planck equation (33) with coupling and with a parameter $q_c=30\%$. With this coupling, a polymer initially at equilibrium at a temperature below T_g can melt in a time that is much shorter than the dominant relaxation time in the initial glassy state.

closest here to the data by Kovacs⁵ corresponds to the value $q_c=30\%$, which we retain in the following. The corresponding evolution of the dominant relaxation time is plotted in Fig. 13. We see indeed that we now observe a temporal asymmetry between cooling and heating a system: the sample melts in a time which is much shorter than its ageing time. In Fig. 14, we plotted the evolution of the distribution of relaxation time during the course of reheating a sample initially at a temperature T_g-15 K to a temperature T_g+20 K. The situation here is that of case (2), that is, the distribution is broader than the equilibrium one. The dominant relaxation time here is thus

$$\tau_\alpha(t) = N_c^{2/3} \tau_{\text{fast}}(t), \quad (47)$$

which acts as a cutoff in the relaxation time distribution at any time during the reequilibration after heating. Physically,

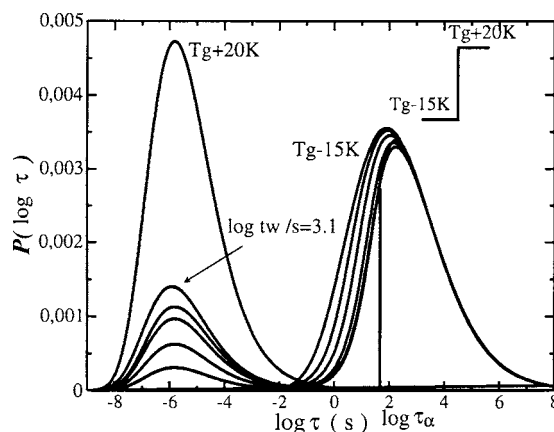


FIG. 14. Relaxation time distribution for PVAc, as a function of time, after heating from equilibrium at T_g-15 K to T_g+20 K. The intermediate times are $\log t_w$ (s)=2.0, 2.5, 2.7, 3.0, and 3.1. For times larger than $10^{3.2}$ s $\ll \tau_\alpha(T_g-15$ K), the distribution of relaxation times coincides with the corresponding equilibrium distribution at the final temperature: The sample has melted. The vertical line corresponds to the cutoff $\tau_\alpha(\tau_w) = N_c^{2/3} \tau_{\text{fast}}$ at time $\log(t_w(s))=3.1$.

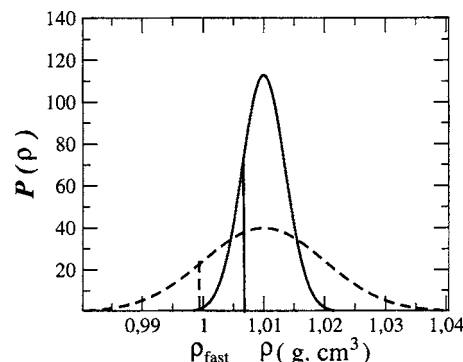


FIG. 15. Equilibrium density fluctuation distributions at fixed average density for two different temperatures: T_g and T_g+50 K (polystyrene data). At high temperature, the distribution widens because the bulk modulus is smaller.

it means that fast subunits melt denser ones in a time that is at most $N_c^{2/3} \tau_{\text{fast}}(q_c)$. This process is responsible for the temporal asymmetry. At short times, the distribution is nearly equal to that at the initial temperature. In this regime, the dominant relaxation time and the volume have not evolved. This regime lasts for a time comparable to the shortest times present in the initial distribution, here about 10 s. After this initial period, fast regions appear within the system: The time $N_c^{2/3} \tau_{\text{fast}}$ becomes shorter than the time corresponding to the 10% densest regions. Then, the fastest regions will melt the slowest ones (see Fig. 3). The time which controls the kinetics of melting is linked to the creation of fast regions in the neighborhood of slow regions, which melt them. That explains the temporal asymmetry.

It is important to note the geometrical nature of the parameter q_c . This is the fraction of fast subunits that is required to melt the densest subunits. Faster subunits—corresponding to a smaller fraction q —are too rare to be able to melt these densest subunits. The fraction we find, 30%, happens to be sufficient to ensure that most of the densest subunits are surrounded by subunits of internal relaxation time $\tau_{\text{fast}} = \tau_{q_c}$ and therefore that most of these dense subunits melt in a time $\tau_{\text{fast}} N_c^{2/3}$. There might remain in the liquid denser subunits surrounded themselves only by slow subunits. The corresponding denser subunits will relax then in a time that can be much longer than τ_α , but the fraction of these very slow subunits is too small to contribute to the α relaxation. They correspond to the dark gray subunits in Fig. 1. The presence of these slow subunits is responsible for the increase of the glass transition temperature in thin films in strong interaction with their substrate.³⁴

The mechanism that we propose is responsible for temporal asymmetry in van der Waals liquids is the following. When one heats a system up—even by maintaining it at fixed average density by applying a pressure—the equilibrium density fluctuation spectrum widens as one can see in Fig. 15. This is also the case for a system that is at atmospheric pressure, with a distribution that is shifted towards smaller values of the density. This wider distribution creates the driving force that pulls the evolution of the actual distribution. This equilibrium distribution is not attained instantaneously of course. The system starts to populate less dense regions

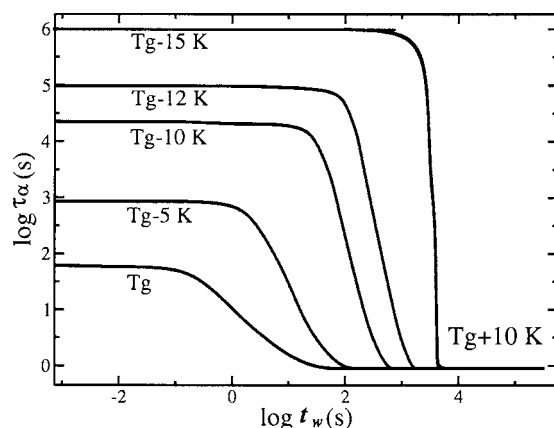


FIG. 16. Dominant relaxation time of PVAc during temperature up jumps to T_g+10 K. The samples are initially at equilibrium at various temperatures: T_g-15 K, T_g-12 K, T_g-10 K, T_g-5 K, and T_g . In all cases the samples melt in a time that is much shorter than the initial dominant relaxation time. On decreasing the initial temperature, melting takes longer.

because this is the faster process. These less dense regions are very fast and melt the denser regions, the relaxation time of which decreases as a consequence: This is the result of what we call the dynamic coupling between fast subunits and denser subunits. Then, the system can expand with a faster rate than the initial relaxation $\tau_\alpha(T_i)$. This is what is observed in Fig. 12 and 13

In Fig. 13, we compared the evolution of the dominant relaxation time during a temperature down jump from T_g+20 K to T_g-15 K and during the course of a temperature up jump from T_g-15 K up to T_g+20 K. In the case of the temperature up jump, one sees that the dominant relaxation time $\tau_\alpha(t)$ remains equal to that of the system at T_g-15 K, i.e., equal to 10^6 s in a first step. In this regime, the dynamics is slow, and macroscopic quantities do not evolve with time. For instance, the volume increases very slowly with the logarithm of the time. This regime lasts up to time $t=10^3$ s. Close to this time, the dominant relaxation time evolves exponentially with time down to the equilibrium value at the considered temperature, i.e., 10^{-2} s: The system has melted. The time it took for the system to melt is much shorter than the dominant relaxation time before heating the system, i.e., 10^6 s. We have seen above that the time it needs to reach equilibrium when cooling a system is equal to the dominant relaxation time at equilibrium whatever the initial temperature. We consider here the time it takes for reaching equilibrium when heating a system, as a function of the initial temperature and of the final temperature. We plotted in Fig. 16 the evolution of the dominant relaxation time after heating up to $T=T_g+10$ K from various temperatures between T_g-15 K and T_g . The time it takes to reach the equilibrium relaxation time at the final temperature is called τ_{rej} . In Fig. 17 we plotted this time as a function of the relaxation time at the initial temperature, $\tau_\alpha(T_i)$. We see that τ_{rej} is orders of magnitude shorter than $\tau_\alpha(T_i)$. The variation can be written in this particular case as

$$t_{\text{rej}} \propto \tau_\alpha(T_i)^\beta \quad \text{with } \beta \approx 0.4. \quad (48)$$

Results are similar when one considers a system initially at

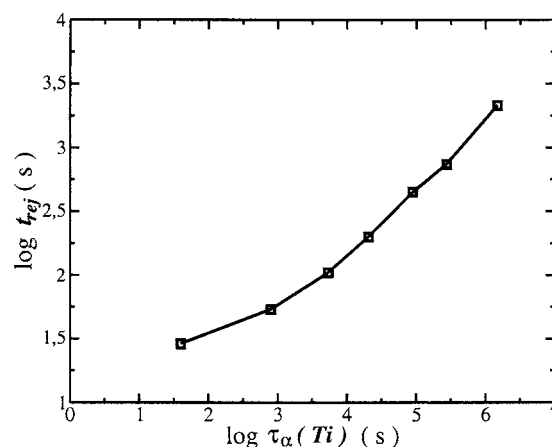


FIG. 17. Rejuvenating time (see text for definition) as a function of the initial dominant relaxation time. The final temperature is T_g+10 K. The rejuvenating time increases with the initial relaxation time but remains much shorter than the former.

very low temperature T_i and which has been allowed to age for a time t_w . The longer the ageing time, the longer τ_{rej} . On the other hand the rejuvenating time is always much shorter than the ageing time: $\tau_{\text{rej}} \ll t_w$.

Now we consider the dependence of the melting time as a function of the relaxation time at the final temperature. At short times, the dominant relaxation time τ_α remains equal to the initial relaxation time at the initial temperature T_g-15 K. After a time τ_{rej} , which depends on the final temperature, the dominant relaxation time $\tau_\alpha(t)$ becomes equal to that at equilibrium at the final temperature. We plotted τ_{rej} as a function of the dominant relaxation time at the final temperature, $\tau_\alpha(T_f)$, in Fig. 18. The rejuvenating time is much shorter than the initial relaxation time $\approx 10^6$ s. The time τ_{rej} decreases when increasing the final temperature. Thus we see that the kinetics for equilibrating a system after heating depends on both the initial and final states, in contrast to the case of cooling. In the latter situation, the time to reach equilibrium depends only on the final state. This asymmetry can be clearly seen when one plots the evolution of the volume of a sample which reaches equilibrium at a given temperature, e.g., T_g , when the system is cooled down (respectively,

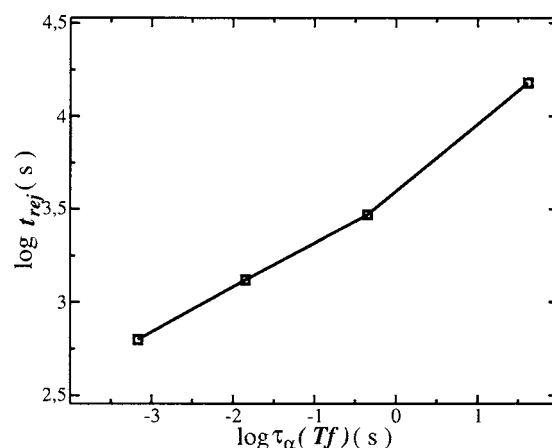


FIG. 18. Rejuvenating time as a function of the dominant relaxation time in the final state. The initial temperature is T_g-15 K. The rejuvenating time increases with the final relaxation time and is larger than the former.

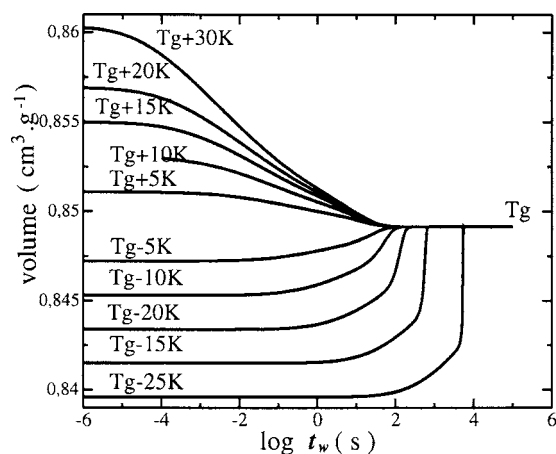


FIG. 19. Variation of PVAc sample volume, as a function of time after heating and after quenching. In the case of quenching the initial temperatures are T_g+5 K, T_g+10 K, T_g+15 K, and T_g+30 K, and the quenching temperature is T_g . In the case of heating, the initial temperatures are T_g-25 K, T_g-20 K, T_g-15 K, T_g-10 K, and T_g-5 K and the samples are heated up to T_g . The samples were initially at equilibrium at the respective temperatures. The evolution of the volume plotted here corresponds to the slow modes associated with α relaxation. This contribution is proportional to the difference of thermal expansion coefficient $\alpha_l - \alpha_g$. The fast mode contribution (proportional to α_g) takes place at much shorter times (not shown).

heated up) from temperatures above (respectively, below) T_g . We plotted such evolutions in Fig. 19. The logarithmic decrease of the volume after cooling has been described.^{5,72,75,76,78} In the case of PVAc, the value measured by Kovacs for temperature down jumps of order of 10 K or more is typically $dv/d \log t \approx (0.8-1.0) \times 10^{-3} \text{ cm}^3 \text{ g}^{-1}$. One can measure the corresponding values in Fig. 19 for temperature jumps down to T_g . One finds 0.8×10^{-3} , 1.0×10^{-3} , 1.3×10^{-3} , and $1.6 \times 10^{-3} \text{ cm}^3 \text{ g}^{-1}$ for initial temperatures, respectively, of T_g+10 K, T_g+15 K, T_g+20 K, and T_g+30 K.

The approach towards equilibrium when changing the temperature such as in Fig. 19 has been the subject of some debate.^{8,81-83} Kovacs *et al.*⁸ introduced an effective relaxation time τ_{eff} to characterize it:

$$\tau_{\text{eff}}^{-1} = -\frac{1}{\delta} \frac{d\delta}{dt}, \quad (49)$$

where δ is the difference between the volume at time t and the volume at equilibrium. We plotted the effective Kovacs τ in Fig. 20 as a function of time, with the same data as those of Fig. 19. At intermediate times, these effective times differ, but at long times they converge towards a time comparable to 1 s, which is the dominant relaxation time at the final temperature. Thus, at intermediate times, there is a so-called Kovacs gap, but at long times the gap disappears: The very final approaches are equivalent, whatever the initial temperature. In Fig. 21, we see that the gap closes when the value of δ is of order of $10^{-4}-10^{-5}$, which is compatible with a recent interpretation of Kovacs's data.⁸³ Our interpretation is the following. At intermediate times, the dynamics depends on the history of the systems: The larger the initial temperature, the faster the evolution. However, at long times, the history of the systems has been erased, and the systems are very

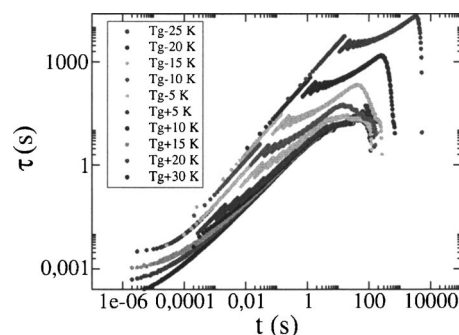


FIG. 20. Kovacs relaxation time [Eq. (49)] obtained from data of Fig. 19 as a function of time after heating or quenching the samples. From top to bottom, the initial temperatures are T_g-25 K, T_g-20 K, T_g-15 K, T_g-10 K, T_g-5 K, T_g , T_g+5 K, T_g+10 K, T_g+15 K, T_g+20 K, and T_g+30 K. At intermediate times, a gap in the values of the effective relaxation time corresponding to different initial states persists. During the very final relaxation to equilibrium, the different effective relaxation times converge.

close to the equilibrium state at the final temperature, here T_g . When the systems are sufficiently close to this state, linear theory applies, and τ_{eff} becomes equal to τ_α at the final temperature.

C. Kovacs effect

Kovacs and other authors^{7,74,75,77} have shown that the evolution of a system when it is heated up depends on its history when the initial state is out of equilibrium. In particular, these authors have shown that the evolution of the volume can be nonmonotonous after a temperature up jump. In Fig. 22 we plotted the evolution of the volume of samples heated up at different temperatures. The samples have aged at a temperature T_g-30 K for 10^5 s. At short times, the volume does not vary. Then, we can distinguish three different situations according to the temperature T_f . At high T_f , the volume increases monotonously before reaching the equilibrium value at temperature T_f . The polymer melts in a time which is much shorter than the ageing time t_w . For intermediate temperatures T_f , for which the equilibrium volume is close to that of the aged sample, the evolution of the volume

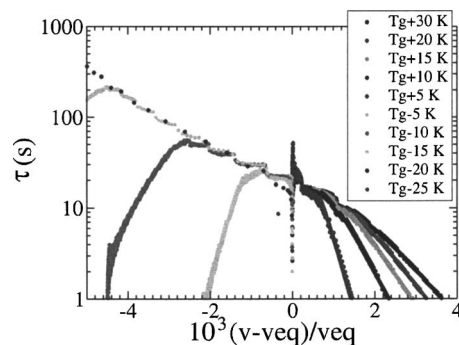


FIG. 21. Kovacs relaxation time (data are from Fig. 19) as a function of the relative difference of the volume to equilibrium. A negative difference corresponds to heating while a positive departure corresponds to quenches. The initial temperatures are, from left to right; T_g-25 K, T_g-20 K, T_g-15 K, T_g-10 K, T_g-5 K, T_g , T_g+5 K, T_g+10 K, T_g+15 K, T_g+20 K, and T_g+30 K. Close to equilibrium at the final temperature, the effective relaxation times τ_{eff} corresponding to different initial temperatures differ. This gap in τ_{eff} vanishes for relative distances to the equilibrium smaller than a few 10^{-4} .

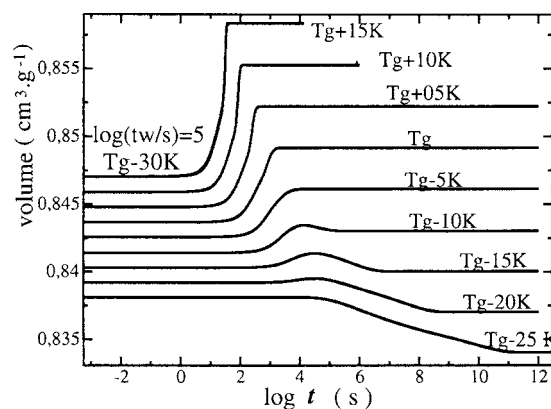


FIG. 22. Variation of the volume for a PVAc sample after heating. The initial states are nonequilibrium ones: The samples have aged for $\log t_w(s)=5$ at temperature T_g-30 K. The final temperatures are, respectively, T_g-20 K, T_g-15 K, T_g-10 K, T_g-5 K, and T_g and T_g+5 K, T_g+10 K, and T_g+15 K. The evolution of the volume may be nonmonotonous depending on the difference between the initial and the final volumes. The difference for the volumes of the different samples at short time is due to the contribution of the fast modes, which is proportional to $\alpha_g \Delta T$.

is nonmonotonous. The curves display an overshoot at a time t_{\max} . The amplitude of this effect is of order a few thousandths. Note that the time t_{\max} is shorter than the time t_w . In a similar way, one can consider the evolution of systems which have aged for various times. In Fig. 23, we plotted the evolution of the volume after heating systems to T_g-10 K after ageing for various times at T_g-20 K. For systems which have aged for a short time (1 s) at T_g-20 K, the initial volume is large as compared to the equilibrium volume at the temperature after heating, and the evolution of the volume is that of a monotonously decreasing function. Similarly, for systems which have aged for a long time, here 10^5 and 10^6 s, the evolution of the volume is that of a monotonously increasing function. On the other hand, for systems which have aged for an intermediate time scale t_w , such that the volume just before heating is close to the equilibrium value at temperature T_g-10 K, the evolution is nonmonotonous. The volume exhibits an overshoot at a time t_{\max} . For the waiting

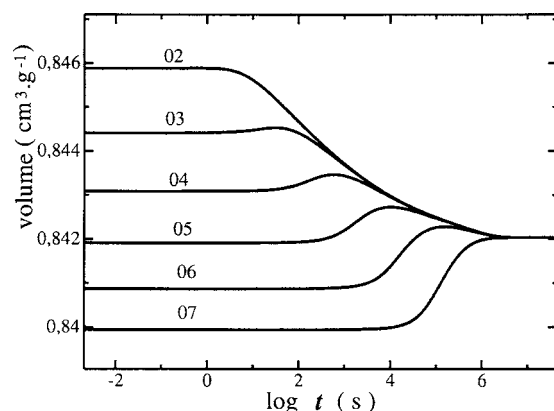


FIG. 23. Volume of a PVAc sample as a function of time during a temperature up jump at T_g-10 K. Before heating, the samples were allowed to age at temperature T_g-30 K for various times t_w : $t_w=10, 100, 1000, 10^4, 10^5, 10^6$, and 10^7 s. The time t_{\max} at which the volume reaches a maximum is found to be proportional to the aging time t_w .

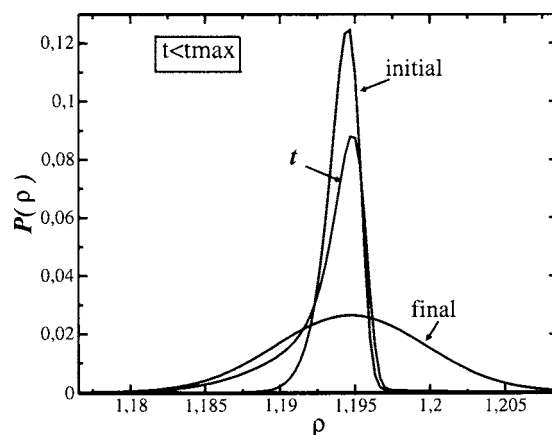


FIG. 24. Density fluctuation distributions (g cm^{-3}) for PVAc. The sample has aged for $\log t_w(s)=7$ at temperature T_g-30 K and is then heated at T_g-20 K. We display the distribution at an intermediate time $\log t(s)=5.5$, which is before the maximum of the volume overshoot. The initial (nonequilibrium) distribution and the equilibrium one at T_g-20 K are also plotted.

times between 10 and 10^4 s, we find that the time scale t_{\max} is proportional to the time spent at low temperature t_w :

$$t_{\max} \propto t_w, \quad (50)$$

which is in agreement with experimental data.⁷⁵ To interpret more precisely this effect, consider Figs. 24 and 25. We consider here a system which has aged for 10^7 s at T_g-30 K and then which is heated up at T_g-20 K. Consider the density fluctuation distribution at a time $t < t_{\max}$ as one can see in Fig. 24. First we note that the initial distribution, i.e., that after 10^7 s ageing, is narrower than the equilibrium distribution at the final temperature. At a time $t < t_{\max}$ the distribution and the initial distribution coincide for the large density fluctuations: The dense regions have not yet had time to relax. On the other hand, the less dense regions corresponding to fast relaxation times have had time to evolve towards the equilibrium distribution at the final temperature. During the course of this process, the density of the sample decreases. At longer time scales ($t > t_{\max}$), the less dense regions are at

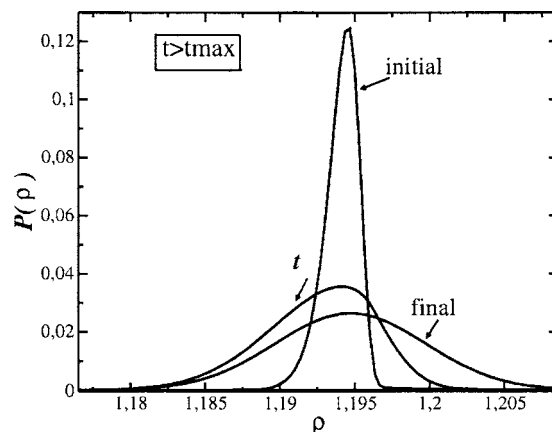


FIG. 25. Density fluctuation distributions for PVAc (g cm^{-3}). The sample has aged for $\log t_w=7$ at temperature T_g-30 K and is then heated at T_g-20 K. One plotted the distribution at an intermediate time $\log t(s)=7$, which is after the maximum of the volume overshoot. The initial (nonequilibrium) distribution and the equilibrium one at T_g-20 K are also shown.

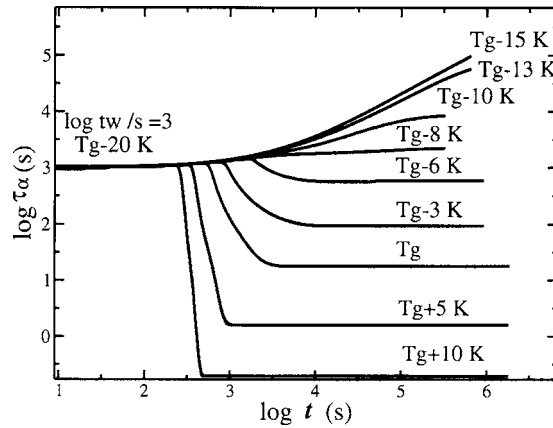


FIG. 26. Dominant relaxation time τ_α during temperature up jumps for a PVAc sample which has aged for a time $t_w=10^3$ s at a temperature T_g-20 K. We do not see any significant nonmonotonicity of this evolution.

equilibrium and no longer evolve, whereas dense regions relax towards the distribution at equilibrium by populating denser regions, as one can see in Fig. 25. As a consequence the density increases before reaching equilibrium. In Fig. 26, we plotted the evolution of the dominant relaxation time τ_α after heating a system which has aged for 10^3 s at T_g-20 K. For all the final temperatures that we consider, we do not observe nonmonotonous evolution of $\tau_\alpha(t)$. When the equilibrium relaxation time at the final temperature is smaller (respectively, larger) than the dominant relaxation time before heating, the evolution of $\tau_\alpha(t)$ is that of a decreasing (respectively, increasing) function.

D. Ageing and small probe diffusion

Thureau and Ediger²³ have measured both the diffusion coefficient D and the rotational correlation time τ_c of small probes during the course of ageing in polymers. Note that the rotational correlation time τ_c is related to a relaxation function $CF(t)$:

$$\tau_c = \int_0^{+\infty} CF(t) dt, \quad (51)$$

whereas the diffusion coefficient is dominated by the fastest relevant relaxation times. Thureau and Ediger observed that $D\tau_c$ displays a nonmonotonous evolution during ageing: The quantity $D\tau_c$ starts to decrease before increasing up to the final value at equilibrium. We recall our interpretation for probe diffusion. D is proportional to the longest times with which it interacts at any time,

$$D \propto \tau_{\text{trans}}. \quad (52)$$

On the other hand, one has

$$\tau_c \simeq \tau_\alpha. \quad (53)$$

Thus, the quantity $D\tau_c$ is a measure of the breadth of the distribution of relaxation times:

$$\log D\tau_c = \log \tau_\alpha - \log \tau_{\text{trans}} + \kappa, \quad (54)$$

where κ is related to the value of $\log D\tau_c$ at high temperature. The nonmonotonous evolution of $\log D\tau_c$ is thus related

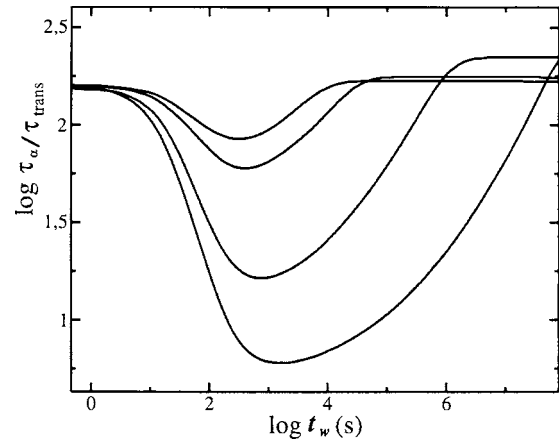


FIG. 27. The quantity $\log(\tau_\alpha/\tau_{\text{trans}})$ during temperature down jumps in polystyrene from T_g down to various temperatures, from top to bottom: T_g-3 K, T_g-5 K, T_g-10 K, and T_g-15 K. The quantity $\log(\tau_\alpha/\tau_{\text{trans}})$ is calculated by solving the Fokker-Planck equation and by using Eqs. (34) and (35) with $q=70\%$. For all these temperature down jumps, we observe a nonmonotonous variation of $\log(\tau_\alpha/\tau_{\text{trans}})$, which is more pronounced for lower temperatures.

to the nonmonotonous evolution of the width of the relaxation time distribution (see Fig. 7).

Here, the dominant relaxation time τ_α is equal to the relaxation time given by Eq. (35), whereas τ_{trans} [Eq. (54)] is determined by

$$\int_0^{\tau_{\text{trans}}} P(\tau) d\tau = q, \quad (55)$$

where $P(\tau)$ is the time dependent distribution of relaxation times and q is a probability number which depends on the relative size of the probe and of the scale of dynamical heterogeneities.³³ The evolution of the quantity $\log(\tau_\alpha/\tau_{\text{trans}})$ during, e.g., a temperature jump depends on the value of the parameter q [see Eq. (55)]. In Fig. 27 we plotted the evolution of $\log(\tau_\alpha/\tau_{\text{trans}})$ for temperature down jumps in polystyrene from T_g to various final temperatures and a value of q equal to 70%. We identify four different regimes. At short times t_w , the quantity $\log(\tau_\alpha/\tau_{\text{trans}})$ is equal to the initial value. In a second step, the quantity $\log(\tau_\alpha/\tau_{\text{trans}})$ diminishes. Finally, $\log(\tau_\alpha/\tau_{\text{trans}})$ increases to reach the final equilibrium value. Note then that the value $\log(\tau_\alpha/\tau_{\text{trans}})$ is larger than the initial value because the final distribution of relaxation times is broader than the initial one. Note that for the value $q=70\%$, both the equilibrium values close to T_g of $\log(\tau_\alpha/\tau_{\text{trans}})$ and of the amplitude of the nonmonotonicity of $\log(\tau_\alpha/\tau_{\text{trans}})$ during ageing— ≈ 0.2 decade²³—are comparable to those measured by Thureau and Ediger.

V. CONCLUSION

We have extended here and made more precise a model for the glass transition in van der Waals liquids that we proposed recently.³²⁻³⁴ Note that this model is intended for both polymeric and molecular van der Waals liquids. We have described in detail the process which leads to the so-called α relaxation and proposed that it corresponds to a tiny fraction of molecular jumps. Whereas relatively fast molecules can diffuse over distances of a few hundreds of nanometers dur-

ing an interval of time τ_α —for a four decade wide relaxation time distribution—the 10% or so slowest molecules will jump and change their local environment only once. But *only the latter contribute to the α relaxation* that can be measured in, e.g., mechanical or dielectric experiments. We proposed that the dynamical heterogeneities in van der Waals liquids stem from thermally induced density fluctuations. That results from the strongly nonlinear behavior of the dynamics as a function of the density close to the glass transition. The characteristic size of these heterogeneities results from the competition between two relaxation mechanisms: (1) the individual monomer jump time, which tends to increase sharply in subunits of large density fluctuations, and (2) the density fluctuation relaxation, which is a collective process on the considered scale. Since the smaller the scale, the larger the density fluctuations and the shorter the lifetime of density fluctuations, these two mechanisms result in the building up of the longest relaxation times on a finite scale, which we found to be of about 2–4 nm at T_g .³³

Beyond making these mechanisms more clear, we proposed here a description of ageing and rejuvenating dynamics in van der Waals liquids. The description of the α process that we proposed in Refs. 32 and 33 and made more precise here is at the heart of the corresponding dynamics. This is all the more clear when considering the temporal asymmetry between ageing and rejuvenating. The mechanism that we propose for that is the following. First, when heating a sample, the system starts to populate faster and faster subunits, but for a while, the densest subunits have not changed. Then, the latter dissolve in the more mobile environment by a process of diffusion of the denser subunits in the faster ones. This process involves the same length scale as that of dynamical heterogeneities. This model allowed us to describe in a unified picture the dynamics of ageing and rejuvenating, the Kovacs memory effect, and the main aspects of small probe diffusion in liquids at equilibrium close to T_g Ref. 33 or here in an ageing liquid. Our model is also able to explain—as well as predict some features—the dynamics in thin films close to T_g .³⁴

As mention in the Introduction, it has been proven that the dynamics in liquids, whether polymeric or simple liquids, is not a function of the sole average density but of both the average density and of the temperature,^{53–61} or equivalently of both the pressure and the temperature. The essential point regarding our model is that the dynamics we consider is a function of *the whole spectrum of density fluctuations* on scale N_c . At equilibrium, the latter is a function of both the average density ρ_{eq} and of the temperature, or of both the *temperature and the pressure*. Thus, intrinsically, the equilibrium dynamics predicted by our model is a function of both the temperature and the average density. In addition, our model allows also to calculate the dynamics in out-of-equilibrium situations when the density fluctuation spectrum differs from that at equilibrium. Thus, our model depends, in general, on an infinite set of degrees of freedom. This is consistent with the Kovacs model which requires a set of degrees of freedom for explaining both temporal asymmetry and memory effects. Indeed, the latter properties rule out in any case the possibility of the dynamics depending on a

single parameter. Our model just proposes here a microscopic description of this set of degrees of freedom and how they are coupled.

We do it in the case of van der Waals liquids, for which we assume that there is no energy barriers. At this stage, let us mention that the most frequent interpretation of experimental results regarding the dependence of the dynamics as a function of the two parameters T and ρ_{eq} is that the part that cannot be accounted for by the average density ρ_{eq} is entirely due to energy barriers. Our model shows that it is not necessarily true. For instance, changing the temperature at fixed density results in a change of the density fluctuation spectrum which results, within our picture, in a change of the dynamics, as we have seen in Fig. 15 and related discussion. In many liquids, though, energy barriers exist. For instance, in the case of polymers, the persistence length might depend on temperature because of activated conformational motions along the backbone. There are also couplings between α relaxation and activated processes such as β processes associated with side group motions not taken into account here. However, quantifying the respective role of density fluctuations on one hand and that of such activated processes on the other hand requires taking into account the relaxation mechanisms described here. A particularly important point, however, is that in liquids that are as close as possible to a van der Waals liquid, Casalini *et al.*,⁵⁸ Roland and Casalini,⁵⁹ and Paluch *et al.*^{60,61} have shown that the most important parameter is the density rather than the temperature. We expect this to be all the more true when taking the relaxation mechanisms described here into account. This will be presented in a forthcoming publication.⁸⁴

APPENDIX: RESOLUTION OF THE FOKKER-PLANCK EQUATION

To solve the Fokker-Planck equation, we discretize the phase space. The density space ρ is then divided in n sites i ($1 \leq i \leq n$). We define the probability of occupancy of the site i by

$$p(i) = \int_{\rho(i)}^{\rho(i+1)} p(\rho) d\rho, \quad (A1)$$

where $p(\rho)$ designs the density probability of the density and $\rho(i)$ the density associated with site i . One has

$$\sum_i P(i) = 1. \quad (A2)$$

To obtain the evolution equation for $P(i)$, we use the following relation:

$$P(i) = p(\rho_i) \Delta\rho, \quad (A3)$$

where $\Delta\rho = \rho(i+1) - \rho(i)$. We deduce

$$\begin{aligned} & \frac{\partial}{\partial \rho} \gamma(\rho) p_{\text{eq}}(\rho) \frac{\partial}{\partial \rho} \left(\frac{P}{p_{\text{eq}}} \right) \\ &= (\Delta \rho)^{-3} \left[\gamma(i+1) P_{\text{eq}}(i+1) \left(\frac{P}{P_{\text{eq}}}(i+1) - \frac{P}{P_{\text{eq}}}(i) \right) \right. \\ & \quad \left. - \gamma(i) P_{\text{eq}}(i) \left(\frac{P}{P_{\text{eq}}}(i) - \frac{P}{P_{\text{eq}}}(i-1) \right) \right], \quad (\text{A4}) \end{aligned}$$

where we denote by $\gamma(i)$ the quantity $\gamma(\rho(i))$. We obtain

$$\begin{aligned} \frac{dP(i)}{dt} &= (\Delta \rho)^{-2} \left[\gamma(i+1) P(i+1) - \gamma(i+1) \frac{P_{\text{eq}}(i+1)}{P_{\text{eq}}(i)} P(i) \right. \\ & \quad \left. - \gamma(i) P(i) + \gamma(i) \frac{P_{\text{eq}}(i)}{P_{\text{eq}}(i-1)} P(i-1) \right]. \quad (\text{A5}) \end{aligned}$$

This equation has the general form of a master equation:

$$\begin{aligned} \frac{dP(i)}{dt} &= W_{i+1,i} P(i+1) - W_{i,i+1} P(i) - W_{i,i-1} P(i) \\ & \quad + W_{i-1,i} P(i-1), \quad (\text{A6}) \end{aligned}$$

where the transition rates $W_{i,j}$ satisfy the relation

$$\begin{aligned} W_{i+1,i} P_{\text{eq}}(i+1) &= W_{i,i+1} P_{\text{eq}}(i) \text{ and } W_{i,i-1} P_{\text{eq}}(i) \\ &= W_{i-1,i} P_{\text{eq}}(i-1). \quad (\text{A7}) \end{aligned}$$

In this picture, aging corresponds to the diffusion of particles in the density phase space. The master equation (A5) can be written in the form

$$\frac{dP}{dt} = -WP, \quad (\text{A8})$$

where P is an n -component vector. The i th element is equal to $P(i)$ and W is an $N \times N$ tridiagonal matrix. This differential equation is solved by using a semi-implicit scheme.⁸⁵

¹M. D. Ediger, C. A. Angell, and S. R. Nagel, J. Phys. Chem. **100**, 13200 (1996).

²C. A. Angell, Science **267**, 1924 (1995).

³J. D. Ferry, *Viscoelastic Properties of Polymers* (Wiley, New York, 1980).

⁴L. C. E. Struik, *Physical Aging in Amorphous Polymers and Other Materials* (Elsevier, Amsterdam, 1978).

⁵A. J. Kovacs, J. Polym. Sci. **30**, 131 (1958).

⁶G. Braun and A. J. Kovacs, Phys. Chem. Glasses **4**, 152 (1963).

⁷A. J. Kovacs, Fortsch. Hochpolym.-Forsch. **3**, 394 (1963).

⁸A. J. Kovacs, J. J. Aklonis, J. M. Hutchinson, and A. R. Ramos, J. Polym. Sci., Polym. Phys. Ed. **17**, 1097 (1979).

⁹K. Schmidt-Rohr and H. W. Spiess, Phys. Rev. Lett. **66**, 3020 (1991).

¹⁰U. Tracht, M. Wilhelm, A. Heuer, H. Feng, K. Schmidt-Rohr, and H. W. Spiess, Phys. Rev. Lett. **81**, 2727 (1998).

¹¹S. A. Reinsberg, X. H. Qiu, M. Wilhelm, H. W. Spiess, and M. D. Ediger, J. Chem. Phys. **114**, 7299 (2001).

¹²M. T. Cicerone, F. R. Blackburn, and M. D. Ediger, Macromolecules **28**, 8224 (1995).

¹³C.-Y. Wang and M. D. Ediger, Macromolecules **30**, 4770 (1997).

¹⁴M. T. Cicerone, P. A. Wagner, and M. D. Ediger, J. Phys. Chem. B **101**, 8727 (1997).

¹⁵C.-Y. Wang and M. D. Ediger, J. Phys. Chem. B **103**, 4177 (1999).

¹⁶C.-Y. Wang and M. D. Ediger, J. Chem. Phys. **112**, 6933 (2000).

¹⁷Y. Hwang, T. Inoue, P. A. Wagner, and M. D. Ediger, J. Polym. Sci., Part B: Polym. Phys. **38**, 68 (2000).

¹⁸F. Fujara, B. Geil, H. Sillescu, and G. Fleischer, Z. Phys. B: Condens. Matter **88**, 195 (1992).

¹⁹A. Tölle, H. Schober, J. Wuttke, O. G. Randl, and F. Fujara, Phys. Rev. Lett. **80**, 2374 (1998).

²⁰I. Chang, F. Fujara, B. Geil, G. Heuberger, T. Mangel, and H. Sillescu, J.

Non-Cryst. Solids **172–174**, 248 (1994).

²¹C. T. Thurau and M. D. Ediger, J. Polym. Sci., Part B: Polym. Phys. **40**, 2463 (2002).

²²T. Sasaki, A. Shimizu, T. H. Mourey, C. T. Thurau, and M. D. Ediger, J. Chem. Phys. **119**, 8730 (2003).

²³C. T. Thurau and M. D. Ediger, J. Chem. Phys. **118**, 1996 (2003).

²⁴M. K. Mapes, S. F. Swallen, and M. D. Ediger, J. Phys. Chem. B **110**, 507 (2006).

²⁵B. Schiener, R. Böhmer, A. Loidl, and R. V. Chamberlin, Science **274**, 752 (1996).

²⁶S. Weinstein and R. Richert, J. Chem. Phys. **123**, 224506 (2005).

²⁷W. Huang and R. Richert, J. Chem. Phys. **124**, 164510 (2006).

²⁸R. Richert, J. Chem. Phys. **113**, 8404 (2000).

²⁹H. Sillescu, J. Non-Cryst. Solids **243**, 81 (1999).

³⁰M. D. Ediger, Annu. Rev. Phys. Chem. **51**, 99 (2000).

³¹R. Richert, J. Phys.: Condens. Matter **14**, R703 (2002).

³²D. Long and F. Lequeux, Eur. Phys. J. E **4**, 371 (2001).

³³S. Merabia and D. Long, Eur. Phys. J. E **9**, 195 (2002).

³⁴S. Merabia, P. Sotta, and D. Long, Eur. Phys. J. E **15**, 189 (2004).

³⁵J. L. Keddie, R. A. L. Jones, and R. A. Cory, Europhys. Lett. **27**, 59 (1994).

³⁶J. A. Forrest, K. Dalnoki-Veress, J. R. Stevens, and J. R. Dutcher, Phys. Rev. Lett. **77**, 2002 (1996); **77**, 4108 (1996).

³⁷S. Kawana and R. A. L. Jones, Phys. Rev. E **63**, 021501 (2001).

³⁸C. J. Ellison and J. M. Torkelson, Nat. Mater. **2**, 695 (2003).

³⁹Y. Grohens, M. Brogly, C. Labbe, M.-O. David, and J. Schultz, Langmuir **14**, 2929 (1998).

⁴⁰J. Berriot, H. Montès, F. Lequeux, D. Long, and P. Sotta, Macromolecules **35**, 9756 (2002).

⁴¹J. Berriot, H. Montès, F. Lequeux, D. Long, and P. Sotta, Europhys. Lett. **64**, 50 (2003).

⁴²F. H. Stillinger and J. A. Hodgson, Phys. Rev. E **50**, 2064 (1994).

⁴³X. Xia and P. G. Wolynes, J. Phys. Chem. B **105**, 6570 (2001).

⁴⁴G. S. Grest and M. H. Cohen, Adv. Chem. Phys. **48**, 455 (1981).

⁴⁵W. Götze and L. Sjögren, Rep. Prog. Phys. **55**, 241 (1992).

⁴⁶G. Tarjus and D. Kivelson, *Jamming and Rheology: Constrained Dynamics on Microscopic and Macroscopic Scales*, edited by S. Edwards, A. Liu, and S. Nagel (Taylor & Francis, London, 2001).

⁴⁷R. Yamamoto and A. Onuki, Phys. Rev. Lett. **81**, 4915 (1998).

⁴⁸C. Donati, J. F. Douglas, W. Kob, S. J. Plimpton, P. H. Poole, and S. C. Glotzer, Phys. Rev. Lett. **80**, 2338 (1998).

⁴⁹I. M. Hodge and A. R. Berens, Macromolecules **15**, 762 (1982).

⁵⁰C. T. Moynihan, P. B. Macedo, C. J. Montrose *et al.*, Ann. N.Y. Acad. Sci. **279**, 15 (1976).

⁵¹R. W. Rendell, K. L. Ngai, G. R. Fong, and J. J. Aklonis, Macromolecules **20**, 1070 (1987).

⁵²G. Diezemann, J. Chem. Phys. **123**, 204510 (2005).

⁵³T. Atake and C. A. Angell, J. Phys. Chem. **83**, 3218 (1979).

⁵⁴G. D. Patterson, J. R. Stevens, and P. J. Carroll, J. Chem. Phys. **77**, 622 (1982).

⁵⁵G. Fytas, Th. Dorfmler, and C. H. Wang, J. Phys. Chem. **87**, 5041 (1983).

⁵⁶M. Naoki, H. Endou, and K. Matsumoto, J. Phys. Chem. **91**, 4169 (1987).

⁵⁷D. M. Colucci, G. B. McKenna, J. J. Filliben, A. Lee, D. B. Curliss, K. B. Bowman, and J. D. Russell, J. Polym. Sci., Part B: Polym. Phys. **35**, 1561 (1997).

⁵⁸R. Casalini, M. Paluch, and C. M. Roland, J. Chem. Phys. **118**, 5701 (2003).

⁵⁹C. M. Roland and R. Casalini, Macromolecules **36**, 1361 (2003).

⁶⁰M. Paluch, C. M. Roland, R. Casalini, G. Meier, and A. Patkowski, J. Chem. Phys. **118**, 4578 (2003).

⁶¹M. Paluch, R. Casalini, A. Patkowski, T. Pakula, and C. M. Roland, Phys. Rev. E **68**, 031802 (2003).

⁶²J. E. Mark, *Physical Properties of Polymers Handbook* (American Institute of Physics, Woodbury, NY, 1996).

⁶³J. E. McKinney and M. Goldstein, J. Res. Natl. Bur. Stand. **78A**, 331 (1974).

⁶⁴D. J. Plazek, Polym. J. (Tokyo, Jpn.) **12**, 43 (1980).

⁶⁵D. J. Plazek, J. Polym. Sci., Polym. Phys. Ed. **20**, 729 (1982).

⁶⁶E. R. Weeks, J. C. Crocker, A. C. Levitt, A. Schofield, and D. A. Weitz, Science **287**, 287 (2000).

⁶⁷G. W. Scherer, *Relaxation in Glass and Composites* (Wiley, New York, 1986).

- ⁶⁸R. E. Robertson, J. Polym. Sci., Polym. Symp. **63**, 173 (1978).
- ⁶⁹N. G. McCrum, B. E. Read, and G. Williams, *Anelastic and Dielectric Effects in Polymeric Solids* (Dover, New York, 1967).
- ⁷⁰B. J. Berne and R. Pecora, *Dynamic Light Scattering* (Wiley, New York, 1976).
- ⁷¹A. Brodin, R. Bergman, J. Mattsson, and E. A. Rössler, Eur. Phys. J. B **36**, 349 (2003).
- ⁷²S. L. Simon, J. W. Sobieski, and D. J. Plazek, Polymer **42**, 2555 (2001).
- ⁷³P. Bernazzani and S. L. Simon, J. Non-Cryst. Solids **307–310**, 470 (2002).
- ⁷⁴K. Adachi and T. Kotaka, Polym. J. (Tokyo, Jpn.) **14**, 959 (1982).
- ⁷⁵S. Hozumi, T. Wakabayashi, and K. Sugihara, Polym. J. (Tokyo, Jpn.) **1**, 632 (1970).
- ⁷⁶H. H.-D. Lee and F. J. McGarry, Polymer **34**, 4267 (1993).
- ⁷⁷R. Greiner and F. R. Schwartl, Rheol. Acta **23**, 378 (1984).
- ⁷⁸J. M. Hutchinson, Prog. Polym. Sci. **20**, 703 (1995).
- ⁷⁹M. Doi and S. F. Edwards, *The Theory of Polymer Dynamics* (Oxford University Press, Oxford, 1986).
- ⁸⁰S. R. de Groot and P. Mazur, *Non-Equilibrium Thermodynamics* (Dover, New York, 1984).
- ⁸¹C. E. Struik, Polymer **38**, 4677 (1996).
- ⁸²C. A. Angell, K. L. Ngai, D. Huang, G. B. McKenna, P. F. McMillan, and S. W. Martin, J. Appl. Phys. **88**, 3113 (2000).
- ⁸³G. B. McKenna, M. G. Vangel, A. L. Rukhin, S. D. Leigh, B. Lotz, and C. Straupe, Polymer **40**, 5183 (1999).
- ⁸⁴S. Merabia and D. Long (unpublished).
- ⁸⁵W. H. Press, S. A. Teukolsky, W. T. Vetterling, and B. P. Flannery, *Numerical Recipes in Fortran* (Cambridge University Press, Cambridge, 1992), Chap. 16, p. 735.